İSTANBUL TECHNICAL UNIVERSITY ★ INSTITUTE OF SCIENCE AND TECHNOLOGY

ENERGY CONCEPT IN EARTHQUAKE-RESISTANT DESIGN

M.Sc. Thesis by

Ali RUZİ

Department : Civil Engineering

Programme: Structural Engineering

May 2003

İSTANBUL TECHNICAL UNIVERSITY ★ INSTITUTE OF SCIENCE AND TECHNOLOGY

ENERGY CONCEPT IN EARTHQUAKE-RESISTANT DESIGN

M.Sc. Thesis by

Ali RUZİ

(501991406)

Date of submission: May 2, 2003

Date of defence examination: May 31, 2003

Supervisor (Chairman): Assoc. Prof. Dr. A. Necmettin GÜNDÜZ

Examining Committee: Prof. Dr. Zekai CELEP (İ.T.Ü.)

Prof. Dr. Zekeriya POLAT (Y.T.Ü.)

MAY 2003

İSTANBUL TEKNİK ÜNİVERSİTESİ ★ FEN BİLİMLERİ ENSTİTÜSÜ

DEPREME DAYANIKLI YAPI TASARIMINDA ENERJİ KAVRAMI

YÜKSEK LİSANS TEZİ

Ali RUZİ
(501991406)

Tezin Enstitüye Verildiği Tarih : 2 Mayıs 2003
Tezin Savunulduğu Tarih : 31 Mayıs 2003

Tez Danışmanı : Doç. Dr. A. Necmettin GÜNDÜZ
Diğer Jüri Üyeleri Prof. Dr. Zekai CELEP (İ.T.Ü.)
Prof. Dr. Zekeriya POLAT (Y.T.Ü.)

MAYIS 2003

PREFACE

As a powerful approach in the performance-based design which is the main issue in structural analysis at present, energy concept is being extensively studied. Thanks to the instruction of my supervisor, energy concept in earthquake-resistant design is decided to be the topic of this study. Because the application range of this topic is so wide, it is not possible to cover it comprehensively in a study like this. As can be seen within the thesis, only the preliminary study of the topic is presented here.

I am highly grateful to my supervisor Assoc. Prof. Dr. A. Necmettin GÜNDÜZ for his useful instruction and sincere help throughout the period of the thesis as well as the class session. It was kind of him to lead me to the relating resources. I am also grateful to other professors in the department who have taught me the necessary knowledge of the major which enables me to prepare this study. All their contributions to my professional education are greatly appreciable. At last, I thank the Republic of Turkey and the people that have supported me during my master study at İstanbul Technical University.

May 2003 Ali RUZİ

CONTENTS

ABBREVIATIONS

SDF	single-degree-of-freedom system
MDF	multi-degree-of-freedom system
RMS	root-mean-square of the ground acceleration
PGA	peak ground acceleration
PGV	peak ground velocity
SIDRS	smoothed inelastic design response spectra
SEDRS	smoothed elastic design response spectra
IRS	inelastic response spectra

FIGURES

SYMBOLS

Part 1

E_i	input energy to the structure
u_m	maximum response deformation in the elastoplastic system
u_y	yield deformation
T	vibration period
m	mass

Part 2

c	viscous damping coefficient
k	stiffness
f_s	restoring force
t	time
u_t	total displacement
u	relative displacement
u_g	earthquake ground displacement
$\dot{u}_t$	total velocity
$\dot{u}$	relative velocity
$\dot{u}_g$	ground velocity
$\ddot{u}_t$	total acceleration
$\ddot{u}$	relative acceleration
$\ddot{u}_g$	ground accelerations
E_k	kinetic energy
E_d	damping energy
E_a	absorbed energy by structures
E_s	elastic strain energy
E_h	hysteretic or plastic or yielding energy
E'_k	relative kinetic energy
E'_i	relative input energy
T_n	natural vibration period
ξ	damping coefficient
f_y	yield force

u_0	peak deformation
f_0	peak force
p	dynamic force exerted on a structure
p_{eff}	effective dynamic force
ω_D	cyclic frequency of damped system
ω_n	natural cyclic frequency of undamped system
u_y	yield deformation
$\bar{f}_y$	normalized yield strength of an elastoplastic system
R_y	the yield reduction factor
u_m	absolute maximum deformation of elastoplastic system
μ	ductility factor
v_e	the equivalent input energy velocity
$\lvert F(\omega)\rvert$	the Fourier amplitude spectrum
$[m]$	the diagonal mass matrix of a MDF system
$[c]$	the diagonal viscous damping matrix
$\{f_s\}$	the restoring force vector
$\{u\}$	the relative displacement vector
$\{\phi\}$	displacement shape vector or mode shape of MDF system
$\delta(t)$	the lateral displacement at the roof level of MDF system
ω^*	the fundamental circular frequency of MDF system
$\{R\}$	the resistance vector of MDF system
E_h^*	the hysteretic energy of the equivalent SDF system
E_s^*	the strain energy of the equivalent SDF system

Part 3

$F(\omega)^*$	the complex conjugate of the Fourier transform of the ground acceleration
$\sigma_{\ddot{u}_g}$	the root-mean-square (RMS) of the ground acceleration
Z	peak factor to estimate the most probable peak-ground-acceleration for a given RMS value
Ω_v	amplification factor to estimate the equivalent input energy velocity by the peak-ground-velocity
Ω_v^*	the peak amplification factor
T_c	the characteristic period of the ground motion
λ	a value to define the spectral shape for period larger than the characteristic period

t_d	the strong ground motion duration
t_0	the length of the digitized accelerogram
γ	Euler constant
c_v	the ratio of the spectral elastic response velocity to peak-ground-velocity in the velocity-controlled (medium) period range
c_a	the ratio of the spectral elastic response acceleration to peak-ground-acceleration in the acceleration-controlled (short) period range
v_{eo}	the peak equivalent input energy velocity
$E_{h,u}$	the allowable plastic energy
n_{eq}	the equivalent number of cycles
F_y	the maximum force
$S_a(T)$	the elastic spectral acceleration
I_D	a seismic index representing the characteristics of earthquake
PGA	the peak ground acceleration
PGV	the peak ground velocity
t_E	the earthquake duration
I_E	the arias intensity
μ_c	the cyclic ductility
T_g	the predominant period of earthquake
T_1	the limit period between the short and the medium period range

Part 4

E_e	the elastic energy
E_D	dissipated energy
E_{es}	the elastic energy supply
E_{ed}	the elastic energy demand
E_{hs}	the hysteretic energy supply
E_{hd}	the hysteretic energy demand
a	normalized pseudoacceleration with respect to g
b	numerical factor for beam proportioning factor
C	elastic seismic coefficient as defined by UBC
F_i	applied force at level i
g	acceleration due to gravity
h_i	height of story level i from ground
I	importance factor as defined by UBC
M	total mass of system
M_{pbi}	plastic moment of beam at level i
M_{pbr}	common reference plastic moment for beams

M_{pc}	plastic moment of columns in first story
S_v	pseudovelocity
T	fundamental period
V_{ei}	earthquake-induced story shear in story level i
V_{en}	earthquake-induced story shear in top story
V_i	story shear in story level i
V_n	story shear in top story
V_y	yield base shear
W	weight
w_i	weight at level i
Z	zone factor as defined by UBC
α	dimensionless parameter used to calculate design base shear
β_i	beam proportioning factor at level i
u_m	maximum displacement
u_y	yield displacement
θ_p	plastic drift
ϕ	resistance factor
$A(T)$	spectral acceleration coefficient
A_0	effective ground acceleration coefficient
I	building importance factor
$S(T)$	spectrum coefficient
R_a	seismic load reduction factor
V_t	total equivalent base shear

SUMMARY

In this study, the energy concept which is a current issue of study and provides a powerful approach in structural analysis is investigated in four parts consisting of the introductory presentation, analytical and statistical evaluation of energy quantities, and the preliminary knowledge of energy-based seismic design of structures. In Part 1, it is explained that the drawbacks of the conventional earthquake resistant design methodologies generated from the force-based or displacement-based analysis of structures can be eliminated by using energy approach. Additionally, the history of energy theory is presented. In Part 2, analytical evaluation of energy components in the single-degree-of-freedom-systems is explained in the absolute energy equation and the relative energy equation and their properties are compared by a numerical example. Moreover, the analytical procedures for the evaluation of energy quantities in the multi-degree-of-freedom systems are briefly presented. In Part 3, utilizing the results of statistical study, firstly, a procedure for estimating input energy spectra in terms of the total power of the ground acceleration is introduced; secondly, a method based on the evaluation of the equivalent number of cycles associated with the earthquake characteristics is introduced in order to evaluate the hysteretic and input energy spectra. In Part 4, the basic design procedures, principles as well as an energy-based seismic design method using yield mechanism and predetermined deformation are presented.

ÖZET

Bu çalışmada güncel araştırma konusu olan ve yapı analizinde güçlü bir yaklaşım sağlayan enerji kavramı incelenmiştir. Dört bölümden oluşan bu çalışma giriş, enerji miktarlarının analitik ve istatistik yöntemlerle elde edilmesi ve yapıların enerjiye dayalı sismik tasarımı konularını içermektedir. Birinci bölümde yapıların kuvvete veya yerdeğiştirmeye dayalı analizinden meydana gelmiş geleneksel depreme dayanıklı yapı tasarımının güçlükleri anlatılmış ve bu zorlukların enerji yaklaşımı ile aşılabileceği ortaya konmuştur. Ayrıca enerji kavramının oluşum süreci anlatılmıştır. İkinci bölümde tek serbestlik dereceli sistemlerdeki enerji bileşenlerinin analitik olarak elde edilmesi mutlak enerji denklemi ve nispi enerji denklemi şeklinde ifade edilmiş ve özellikleri bir sayısal örnekle karşılaştırılmıştır. Buna ek olarak çok serbestlik dereceli sistemlerdeki enerji değerlerinin elde edilmesi kısaca anlatılmıştır. Üçüncü bölümde istatistik araştırma sonuçlarından yararlanılarak, önce yer ivmesinin toplam gücü cinsinden ifade edilmiş en büyük giriş enerjisini elde eden bir yöntem tanıtılmıştır; sonra deprem özelliklerine bağlı olarak ifade edilmiş eşdeğer çevirim sayısına dayalı, en büyük plastik enerji ve giriş enerjisini elde eden bir yöntem daha tanıtılmıştır. Dördüncü bölümde temel tasarım aşamaları, tasarım ilkeleri ve önceden belirlenmiş akma mekanizması ve yerdeğiştirmesini esas alan bir enerjiye dayalı sismik tasarım yöntemi tanıtılmıştır.

PART 1 INTRODUCTION

Present earthquake-resistant design methodologies and the earthquake damage assessment approaches oriented from the traditional force-based or displacement-based analysis of structures have many shortcomings. These shortcomings can be eliminated by utilizing energy approach which has been developed in several stages by different researchers such as Housner and Akiyama etc.

1.1 Shortcomings of the Conventional Force-Based or Displacement-Based Analysis of Structures

In the analysis of structural systems, two main issues must be considered: the first is the interpretation of the load, such as earthquake ground motions, applied to structures and the objective evaluation of its effects; the second is the evaluation of resistance of structures to such external loading effects [1].

In traditional seismic analysis of structures, the loading effect of the earthquake is represented by static equivalent forces, which are obtained from elastic response spectra representing the relation between the peak ground acceleration and the pseudo-acceleration [2]. In considering the contribution of ductility in a structure, a seismic force reduction factor is utilized to reduce the elastic force demand to the design level. The seismic force reduction factor represents the ductility capacity. However, the effect of duration-related cumulative damage is neglected in this procedure. Another alternative approach, displacement-based design procedure is being developed. Nonetheless, the same drawback still exists [3]. Furthermore, the forces exerted by an earthquake are defined by the elastic and plastic characteristics of the structure. Consequently, the loading effect of the earthquake and the resistance of the structure are coupled, because of which, the seismic design becomes quite complex [2].

1.2 Necessity of Using Energy Concept in Seismic Analysis

In order to eliminate these shortcomings, energy theory has been proposed by researchers. In the energy theory, the total amount of energy exerted by an earthquake, input energy, is considered as the external load and the corresponding resistance of the structure is the energy absorption capacity of the frame [1].

Modern approaches in the seismic design methodologies are established on the definition of performance-based methods for both the design of new structures and the assessment of the seismic capacity of existing structures. In this field, utilizing the energy concept and the energy balance equation enables us to optimize the design and detailing and to define methodologies and techniques for innovative control or protective systems such as base isolation and passive energy dissipation devices in the earthquake-resistant design of new structures or in the seismic retrofitting of existing structures.

Referring to the earthquake demand, different authors consider the input energy E_i as an effective tool in the seismic design pointing out that E_i represents a very stable parameter of the structural response and it hardly depends on the hysteretic properties of the structure. However, it is necessary to observe that a part of the input energy transmitted to structure by an earthquake is dissipated by means of damping whereas another is dissipated by means of the inelastic deformation, which is the hysteretic energy. Only the part of the dissipated energy due to the inelastic deformation contributes to the damage of a structure subjected to the seismic excitation.

Particularly, the energy criterion shows that the structure collapses if it is demanded to dissipate, via inelastic deformations, an amount of energy larger than that supplied. However, it has the limitation to treat the energy dissipated in all the plastic cycles regardless of the amplitude of each cycle. On the other hand, it is experimentally shown that in many cases plastic cycles having a low amplitude do not contribute to the damage. Therefore, it is necessary that only a fraction of the plastic energy be considered to cause damage. Nonetheless, despite the limitation, the energy approach is regarded as a powerful tool in seismic design because of the simplicity and the large experimental background. Furthermore, if the energy demand is supposed to be equal to

the energy dissipated under monotonic loads, the energy criterion represents a lower limit of the response capacity of the structure and, therefore, its application is on safe side leading to a conservative design.

However, reliable assessment of the demand of the dissipated energy that is very dependent on earthquake characteristics forms the base for energy method. This assessment is carried out by means of the evaluation of the input energy by many researchers [4].

One of the significant advantages of representing the loading effect of earthquakes in terms of energy is that the characteristics of ground motions and those of the structure can be dealt with separately, that is, earthquake load effect and structural resistance can be basically uncoupled. The characterization of the loading effect of the earthquake in terms of energy is the basis of the so-called energy-based seismic design methods [2].

On the damage assessment, generally, the damage potential of ground motions is measured by its maximum acceleration or velocity. However, the results from high acceleration and velocity of some recent ground motions show that the relation between the damage potential of earthquakes and the damage to structures is not so. The impulsive acceleration of near fault earthquake and the cyclic effect of far source earthquake cause different damages respectively. Therefore, the dynamic damage potential of ground motions must be evaluated by the response behavior of structures.

The total input energy (energy spectrum) is a representative estimation concept of the damage potential of ground motions, in which the earthquake-resistant capacity of structures is evaluated by means of energy dissipating behavior via viscous damping and inelastic hysteresis loop [5].

1.3 The history of the Energy Theory

Energy theory has the following history of development:

1. Tanahashi conducted an elastic-plastic analysis of buildings subjected to pulse-like artificial ground motions and concluded that the square of the maximum velocity of ground motions can be used as an indicator of the earthquake's destructive force.

2. Housner made a quantitative evaluation of the total amount of energy input that contributes to the building's responses with the use of the velocity response spectra in the elastic system and assumed that the energy input responsible for the damage in the elastic-plastic system is identical to that in the elastic system. Housner verified his hypothesis by examination of several examples of damage. However, these examples were limited to cases of plastic deformation of anchor-bolts in column bases of steel structures and of bracings in the frames for which diagonal bracings with a large slenderness ratio were used for resistance to lateral forces. Housner limited his examinations to these structures because the amount of energy absorbed by the plastic deformation can be easily determined in these structures.

3. Velestos and Newmark conducted a response analysis of the one-mass elastic plastic system. They obtained the ratio of the maximum response deformation in the elastic perfectly plastic system u_m to the maximum response deformation in the elastic system u_y, and suggested the possibility of making an estimate of its upper bound value by assuming the apparent equivalence in strain energy.

4. Penzien drew a similar conclusion through the response analysis of the single-degree-of-freedom system and the multi-degree-of-freedom elastic-plastic system [1].

5. Akiyama showed that the total amount of input energy E_i exerted by a given earthquake on a structure is a very stable parameter, governed primarily by the natural period T and the total mass m, and scarcely by other structural characteristics such as the resistance, damping, hysteretic loop shapes, etc [2].

6. Uang and Bertero have presented the conceptual methodology for earthquake resistant design of reinforced concrete buildings. In this methodology, total input energy, inelastic design response spectra, and energy dissipation obtained through damping energy and hysteretic energy are considered simultaneously, to discuss the damage potential of ground motions and the damage index of structures.

7. Krawinkler and Nassar have presented that ductility and cumulative damage considerations can and should be incorporated explicitly into the design process, and proposed the seismic design procedure using demand spectrum. In this procedure,

demand parameters (strength, ductility, energy) are defined as a quantity that relates seismic input to structural response.

8. Fajfar has applied damage index that is based on maximum displacement and dissipated energy to also consider cumulative damage for evaluating structural damage, and presented examples of inelastic design spectra using equivalent ductility factor corresponding to given damage index [5].

PART 2 THEORETICAL EVALUATION OF SEISMIC ENERGY IN STRUCTURES

Various energy quantities in structures are defined as the work done by the corresponding structural forces such as inertial force, damping force and resisting force. Seismic energies in structures are theoretically evaluated by integrating the dynamic equation of motion in the deformation range. In the energy analysis of single-degree-of-freedom (SDF) systems subjected to earthquake induced ground motions, two types of equations are available in literature. The first approach uses an absolute energy formulation while the second approach uses a relative energy formulation. Both energy formulations can be interpreted as the work done by different forces. For a given ductility ratio, the input energy demands evaluated by using both methods are identical in the intermediate period range, however they are different at large extend for the short and long period ranges [6].

2.1 Evaluation of Energy in Single-Degree-of-Freedom Systems

Energy equations can be evaluated only within the limitation of a linearly elastic-perfectly plastic, elastoplastic briefly, SDF system.

For a viscous damped SDF system subjected to a horizontal earthquake ground motion, the equation of motion can be written as

$$m\ddot{u}_t + c\dot{u} + f_s = 0 \tag{2.1.1}$$

where $m =$ mass, $c =$ viscous damping coefficient, $f_s =$ restoring force, $u_t = u + u_g =$ absolute (or total) displacement of the mass, $u =$ relative displacement of the mass with respect to the ground, and $u_g =$ earthquake ground displacement.

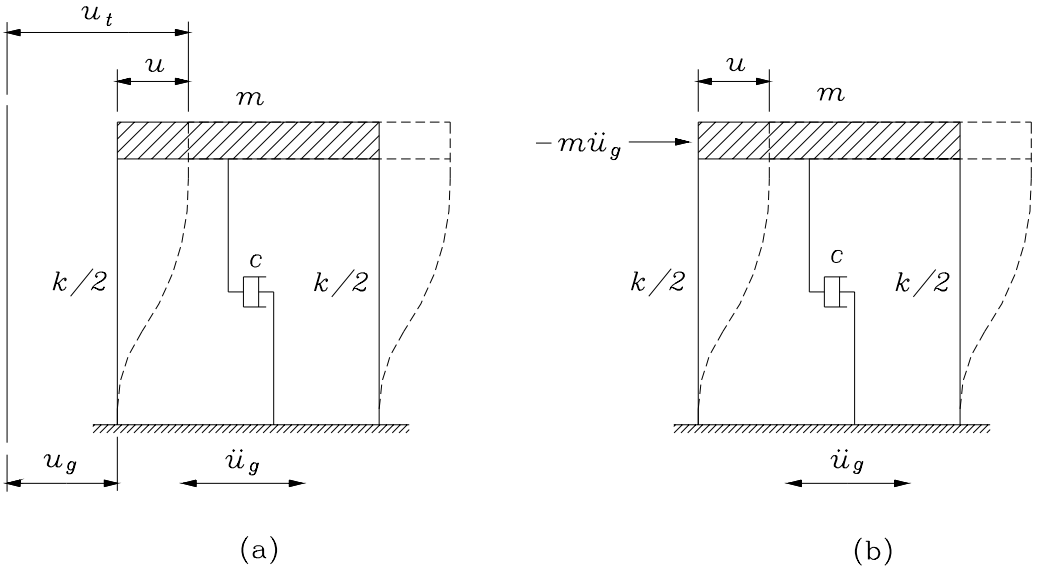

Figure 2.1 Mathematical model of a SDF system subjected to an earthquake ground motion

It should be noted that f_s may be expressed as ku for a linear elastic system where k = stiffness. Substituting $\ddot{u}_t = \ddot{u} + \ddot{u}_g$, Eq. 2.1.1 can be written as

$$m\ddot{u} + c\dot{u} + f_s = -m\ddot{u}_g \tag{2.1.2}$$

Consequently, the structural system in Fig. 2.1a can easily be seen as the equivalent system in Fig. 2.1b with a fixed base and subjected to an effective horizontal dynamic force of magnitude $-m\ddot{u}_g$. Although the relative displacement which both systems undergo is identical, the equations result in the input energy and kinetic energy with different definitions depending on whether Eq. 2.1.1 or Eq. 2.1.2 is used. Corresponding to the specific equation used to derive energy formulation, two kinds of energy formulation can be introduced, i.e. absolute energy formulation and relative energy formulation.

2.1.1 Formulation 1 – Derivation of Absolute Energy Equation

Integrate Eq. 2.1.1 with respect to u from the time that the ground motion excitation starts:

$$\int m\ddot{u}_t du + \int c\dot{u} du + \int f_s du = 0 \tag{2.1.3}$$

Substituting $u = (u_t - u_g)$ in the first term of Eq. 2.1.3, then

$$\int m\ddot{u}_t du = \int m\ddot{u}_t (du_t - du_g) = \int m\frac{d\dot{u}_t}{dt} du_t - \int m\ddot{u}_t du_g = \int m\dot{u}_t d\dot{u}_t - \int m\ddot{u}_t du_g \qquad (2.1.4)$$

$$= \frac{m(\dot{u}_t)^2}{2} - \int m\ddot{u}_t du_g$$

Substituting Eq. 2.1.4 into Eq. 2.1.3 yields

$$\frac{m(\dot{u}_t)^2}{2} + \int c\dot{u}du + \int f_s du = \int m\ddot{u}_t du_g \qquad (2.1.5)$$

The first term of the above equation is the absolute kinetic energy E_k,

$$E_k = \frac{m(\dot{u}_t)^2}{2} \qquad (2.1.6)$$

since the absolute velocity $\dot{u}_t$ is used to calculate the kinetic energy. The second term in Eq. 2.1.5 is the damping energy E_d, which is always non-negative because

$$E_d = \int c\dot{u}du = \int c\dot{u}^2 dt \qquad (2.1.7)$$

The third term in Eq. 2.1.5 is the absorbed energy E_a, which consists of recoverable elastic strain energy E_s and irrecoverable hysteretic or yielding or plastic energy E_h:

$$E_a = \int f_s du = E_s + E_h \qquad (2.1.8)$$

where $E_s(t) = \frac{[f_s(t)]^2}{2k}$ and $E_h(t) = \int f_s(u,\dot{u})du - E_s(t) = \left[\int \dot{u} f_s(u,\dot{u})dt\right] - E_s$ [7].

By definition, the right hand side term in Eq. 2.1.5 is the input energy E_i:

$$E_i = \int (m\ddot{u}_t) du_g \qquad (2.1.9)$$

E_i is defined as the absolute input energy in this formulation. This definition is physically meaningful for that the term $m\ddot{u}_t$ represents the inertia force applied to the structure. The total force applied to the structure foundation is equal to this inertia force

which is composed of restoring force and damping force due to Eq. 2.1.1. Therefore, E_i can be treated as the work done by the total base shear at the foundation on the foundation displacement. Consequently, the absolute energy equation can be written as

$$E_i = E_k + E_d + E_a = E_k + E_d + E_s + E_h \tag{2.1.10}$$

2.1.2 Formulation 2 – Derivation of Relative Energy Equation

Integrate Eq. 2.1.2 with respect to u :

$$\int m\ddot{u}du + \int c\dot{u}du + \int f_s du = -\int m\ddot{u}_g du \tag{2.1.11}$$

It is observed that the second and third term on the left side of the equation are identical to the ones of Eq. 2.1.3 and equal to E_d and E_a respectively. The first term of Eq. 2.1.11 can be written as

$$\int m\ddot{u}du = \int m\frac{d\dot{u}}{dt}du = \int m\dot{u}d\dot{u} = \frac{m(\dot{u})^2}{2}$$

which is the relative kinetic energy E_k' calculated from the relative velocity:

$$E_k' = \frac{m(\dot{u})^2}{2} \tag{2.1.12}$$

The right side term of Eq. 2.1.11 is then defined as the input energy E_i' :

$$E_i' = -\int m\ddot{u}_g du \tag{2.1.13}$$

E_i' is formulated as the relative input energy in this formulation. This definition physically represents the work done by the static equivalent lateral force $-m\ddot{u}_g$ on the equivalent fixed-base system. In other words, it neglects the effect of the rigid body translation of the structure. Consequently, the relative energy equation can be expressed as

$$E_i' = E_k' + E_d + E_a = E_k' + E_d + E_s + E_h \tag{2.1.14}$$

2.2 Comparison of Energy Time Histories

2.2.1 Prerequisite Presentation for Energy Time History

Evaluation of the energy terms requires that the earthquake response analysis of the system be conducted. Because evaluation of energy quantities is limited to the elastoplastic system, it is necessary to obtain inelastic dynamic response of the corresponding system for selected vibration period T_n, damping ratio ξ and yield force f_y. Obviously, we have to determine firstly the response $u(t)$ of the linear system in order to define the peak deformation u_0 and the peak force $f_0 = ku_0$ which are necessary for the inelastic dynamic analysis. Evaluation of the response analysis of a linear system and nonlinear system has been briefly recalled here [7].

2.2.1.1 Response Analysis of a Linear System

The governing equation for an elastic system under the ground motion is

$$m\ddot{u}(t) + c\dot{u}(t) + ku(t) = -m\ddot{u}_g(t) \tag{2.2.1}$$

Deformation response of a linear system to an arbitrary ground motion with zero initial conditions is given by Duhamel's integral with dynamic force $p(t)$ replaced by $p_{eff}(t) = -m\ddot{u}_g(t)$:

$$u(t) = -\frac{1}{\omega_D}\int_0^t \ddot{u}_g(\tau)e^{-\xi\omega_n(t-\tau)}\sin\left[\omega_D(t-\tau)\right]d\tau \tag{2.2.2}$$

By differentiating Eq. 2.2.2 under the integral sign

$$\dot{u}(t) = -\xi\omega_n u(t) - \int_0^t \ddot{u}_g(\tau)e^{-\xi\omega_n(t-\tau)}\cos\left[\omega_D(t-\tau)\right]d\tau \tag{2.2.3}$$

The equation of motion for the system provides us an equation for the acceleration $\ddot{u}^t(t)$

$$\ddot{u}^t(t) = -\omega_n^2 u(t) - 2\xi\omega_n\dot{u}(t) \tag{2.2.4}$$

These integrals can be carried out by numerical ways.

However, integration of equation of motions under arbitrary force can be easily carried out by numerical time-stepping methods available in the literature. Newmark's method has been presented here. Following procedure summarizes Newmark's time-stepping method as it can be implemented on the computer program.

Newmark's method for linear systems:

Special cases

(1) Average acceleration method ($\gamma = \frac{1}{2}$, $\beta = \frac{1}{4}$)

(2) Linear acceleration method ($\gamma = \frac{1}{2}$, $\beta = \frac{1}{6}$)

1.0 Initial calculations

1.1 $\ddot{u}_0 = \frac{p_0 - c\dot{u}_0 - ku_0}{m}$.

1.2 Select Δt.

1.3 $\hat{k} = k + \frac{\gamma}{\beta \Delta t} c + \frac{1}{\beta (\Delta t)^2} m$.

1.4 $a = \frac{1}{\beta \Delta t} m + \frac{\gamma}{\beta} c$; and $b = \frac{1}{2\beta} m + \Delta t \left(\frac{\gamma}{2\beta} - 1 \right) c$.

2.0 Calculations for each time step, i

2.1 $\Delta \hat{p}_i = \Delta p_i + a\dot{u}_i + b\ddot{u}_i$.

2.2 $\Delta u_i = \frac{\Delta p_i}{\hat{k}}$.

2.3 $\Delta \dot{u}_i = \frac{\gamma}{\beta \Delta t} \Delta u_i - \frac{\gamma}{\beta} \dot{u}_i + \Delta t \left(1 - \frac{\gamma}{2\beta} \right) \ddot{u}_i$.

2.4 $\Delta \ddot{u}_i = \frac{1}{\beta (\Delta t)^2} \Delta u_i - \frac{1}{\beta \Delta t} \dot{u}_i - \frac{1}{2\beta} \ddot{u}_i$.

2.5 $u_{i+1} = u_i + \Delta u_i,\ \dot{u}_{i+1} = \dot{u}_i + \Delta \dot{u}_i,\ \ddot{u}_{i+1} = \ddot{u}_i + \Delta \ddot{u}_i.$

3.0 Repetition for the next time step. Replace i by $i+1$ and implement steps 2.1 to 2.5 for the next time step.

2.2.1.2 Response Analysis of a Nonlinear System

The governing equation for an inelastic system under the ground motion is

$$m\ddot{u}(t) + c\dot{u}(t) + f_s(u,\dot{u}) = -m\ddot{u}_g(t) \tag{2.2.5}$$

Force-deformation relation for an inelastic system can be idealized, for convenience, by an elastic-perfectly plastic, elastoplastic briefly, or bilinear force-deformation relation. Under initial loading, this idealized system behaves as linearly elastic system with stiffness k as long as the force does not exceed yield strength f_y. Yielding begins when the force reaches f_y. The deformation at which yielding begins is u_y, the yield deformation. Yielding takes place at constant force i.e. the stiffness is zero. Fig. 2.2 shows a typical cycle of loading, unloading and reloading for an elastoplastic system.

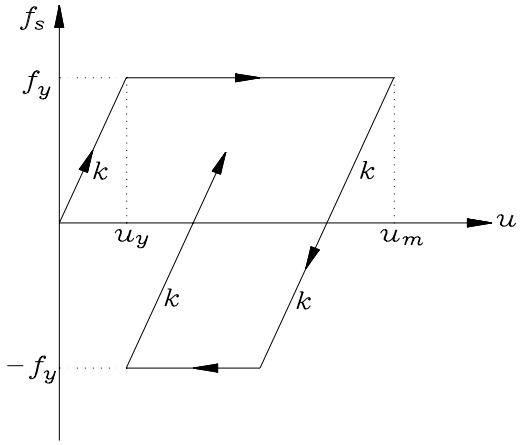

Figure 2.2 Elastoplastic force-deformation relation

The normalized yield strength $\bar{f}_y$ of an elastoplastic system is defined as

$$\bar{f}_y = \frac{f_y}{f_0} = \frac{u_y}{u_0} \tag{2.2.6}$$

where f_0 and u_0 are the peak values of the earthquake-induced resisting force and deformation respectively in the corresponding linear system. f_0 can be explained as the strength at which the structure remains within its linearly elastic limit during the earthquake excitation. It is easy to validate the second part of Eq. 2.2.6 by using $f_y = ku_y$ and $f_0 = ku_0$.

The yield reduction factor R_y which defines an alternative relation between f_y and f_0 is presented as

$$R_y = \frac{f_0}{f_y} = \frac{u_0}{u_y}. \tag{2.2.7}$$

Obviously, R_y is reciprocal of $\bar{f}_y$.

The peak, or absolute (without regard to algebraic sign) maximum, deformation of the elastoplastic system induced by the earthquake excitation is denoted by u_m. The ductility factor μ then can be defined as

$$\mu = \frac{u_m}{u_y}, \tag{2.2.8}$$

which is the normalization of u_m relative to the yield deformation of the system.

The relationship between the peak deformation u_m and u_0 of the elastoplastic and corresponding linear system can be explained by their ratio as

$$\frac{u_m}{u_0} = \mu\bar{f}_y = \frac{\mu}{R_y}. \tag{2.2.9}$$

Dynamic response of an inelastic system is also obtained by using various numerical procedures available in the literature. One of them, Newmark's method has been presented here.

Newmark's method for nonlinear systems:

Special cases

(1) Average acceleration method ($\gamma = \frac{1}{2}$, $\beta = \frac{1}{4}$)

(2) Linear acceleration method ($\gamma = \frac{1}{2}$, $\beta = \frac{1}{6}$)

1.0 Initial calculations

1.1 $\ddot{u}_0 = \frac{p_0 - c\dot{u}_0 - (f_s)_0}{m}$.

1.2 Select Δt.

1.3 $a = \frac{1}{\beta \Delta t} m + \frac{\gamma}{\beta} c$; and $b = \frac{1}{2\beta} m + \Delta t \left(\frac{\gamma}{2\beta} - 1 \right) c$.

2.0 Calculations for each time step, i

2.1 $\Delta \hat{p}_i = \Delta p_i + a\dot{u}_i + b\ddot{u}_i$.

2.2 Determine the tangent k_i.

2.3 $\hat{k}_i = k_i + \frac{\gamma}{\beta \Delta t} c + \frac{1}{\beta (\Delta t)^2} m$.

2.4 Solve for Δu_i from $\hat{k}_i$ and $\Delta \hat{p}_i$ using the iterative procedure.

2.5 $\Delta \dot{u}_i = \frac{\gamma}{\beta \Delta t} \Delta u_i - \frac{\gamma}{\beta} \dot{u}_i + \Delta t \left(1 - \frac{\gamma}{2\beta} \right) \ddot{u}_i$.

2.6 $\Delta \ddot{u}_i = \frac{1}{\beta (\Delta t)^2} \Delta u_i - \frac{1}{\beta \Delta t} \dot{u}_i - \frac{1}{2\beta} \ddot{u}_i$.

2.7 $u_{i+1} = u_i + \Delta u_i$, $\dot{u}_{i+1} = \dot{u}_i + \Delta \dot{u}_i$, $\ddot{u}_{i+1} = \ddot{u}_i + \Delta \ddot{u}_i$.

3.0 Repetition for the next time step. Replace i by $i+1$ and implement steps 2.1 to 2.7 for the next time step.

The procedure to evaluate energy time history for an inelastic SDF system can be summarized as following:

1. Numerically define the ground motion $\ddot{u}_g(t)$.
2. Select the damping ratio ξ for which the energy time history is defined.
3. Select a value for T_n.
4. Determine the response $u(t)$ of the linear system with T_n and ξ equal to the values selected. From $u(t)$ determine the peak deformation u_0 and the peak force $f_0 = ku_0$.
5. Determine the response $u(t)$ of an elastoplastic system with the same T_n and ξ, and yield force $f_y = \bar{f}_y f_0$, with a selected $\bar{f}_y < 1$.
6. Compute the corresponding energy terms by using the obtained response of the elastoplastic system and show them on a plot.

2.2.2 Numerical Example

2.2.2.1 Elastic response analysis of the system with $T_n = 0.2\,\text{sec}$

An elastic SDF system has the following characteristics:

$m = 10142.4 Ns^2/m = 10142.4 kg$, $k = 10 \times 10^6 N/m$, $(\omega_n = 31.4 rad/\text{sec})$, $\xi = 0.05$.

East-West acceleration component of Düzce earthquake recorded at Düzce Meteorology Station in Nov. 12, 1999 is used for this analysis. It is shown in Fig. 2.3. Its peak ground acceleration and magnitude were $0.52g$ and $7.2\,ML$ respectively.

Dynamic responses of this system to the selected ground motion are evaluated below:

Initial calculations

$c = 2\xi m\omega_n = 31847.136$

$u_0 = 0$, $\dot{u}_0 = 0$, $p_0 = 0$

$\ddot{u}_0 = \dfrac{p_0 - c\dot{u}_0 - ku_0}{m} = 0$.

$\Delta t = 0.005$.

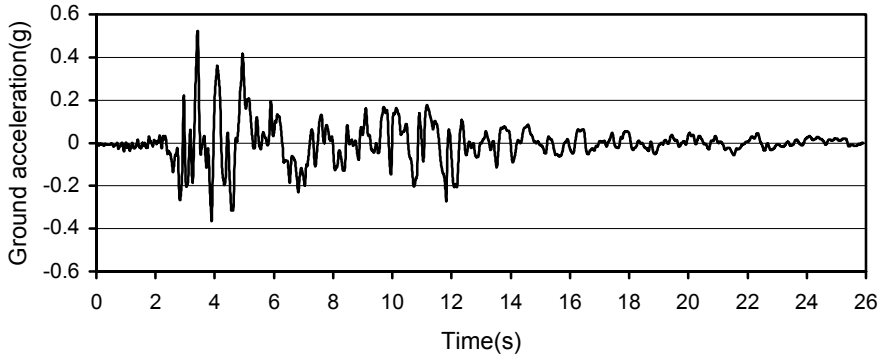

Figure 2.3 Acceleration time history of Düzce earthquake in 1999

Above summarized Newmark's time-stepping method has been implemented on the C program code given at Appendix A.

The deformation response of this system is presented in Fig. 2.4. As seen in the figure, $u_0 = 0.001309m$ at $t = 3.41\text{sec}$ and the corresponding peak resisting force $f_0 = ku_0 = 13.09 \times 10^3 N$.

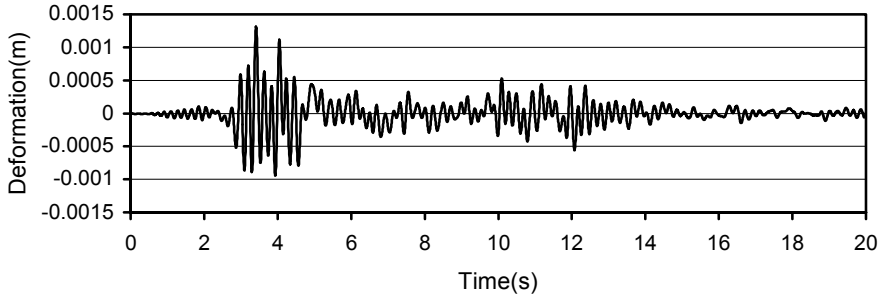

Figure 2.4 Deformation response of the linear system with $T_n = 0.2\text{sec}$ and $\xi = 0.05$

2.2.2.2 Elastic response analysis of the system with $T_n = 5\text{sec}$

An elastic SDF system has the following characteristics:

$m = 63390Ns^2/m = 6338999.55kg$, $k = 10 \times 10^6 N/m$, $(\omega_n = 1.256rad/\text{sec})$, $\xi = 0.05$. Düzce earthquake in 1999 has been selected for the ground motion. Dynamic responses of this system to the selected ground motion have been evaluated below.

Initial calculations

$c = 2\xi m\omega_n = 796178.27$

$u_0 = 0$, $\dot{u}_0 = 0$, $p_0 = 0$

$\ddot{u}_0 = \dfrac{p_0 - c\dot{u}_0 - ku_0}{m} = 0$.

$\Delta t = 0.005$.

By the same C program through corresponding changes, the deformation response of this system is presented in Fig. 2.5. As seen in the figure, $u_0 = 0.16283m$ at $t = 13.63\,\text{sec}$ and the corresponding peak resisting force $f_0 = ku_0 = 1628300N$.

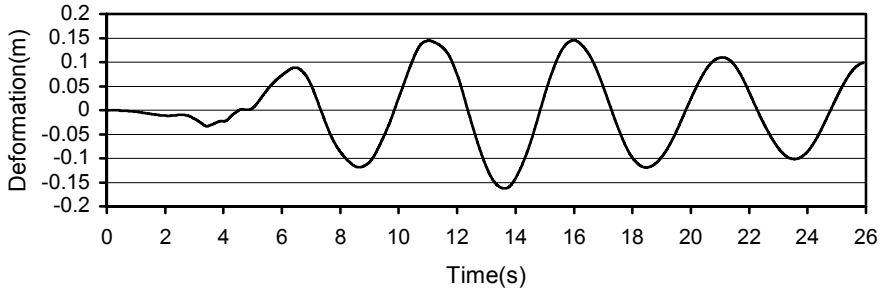

Figure 2.5 Deformation response of the linear system with $T_n = 5\,\text{sec}$ and $\xi = 0.05$

2.2.2.3 Inelastic response analysis of the system with $T_n = 0.2\,\text{sec}$

For the same system, the selected normalized yield strength $\bar{f} = 0.125$, the corresponding yield force $f_y = 1636N$ and the yield deformation $u_y = \dfrac{f_y}{k} = 0.00011636m$.

Initial calculations

$u_0 = 0$, $\dot{u}_0 = 0$, $p_0 = 0$

$\ddot{u}_0 = \dfrac{p_0 - c\dot{u}_0 - k_0u_0}{m} = 0$.

$\Delta t = 0.005$.

Previously summarized Newmark's time-stepping method for the nonlinear system has been implemented on the C program code given at Appendix B.

Deformation response, inelastic resisting force response and the force-deformation relation, hysterics loop, has been shown in Fig. 2.6, Fig. 2.7 and Fig. 2.8 respectively.

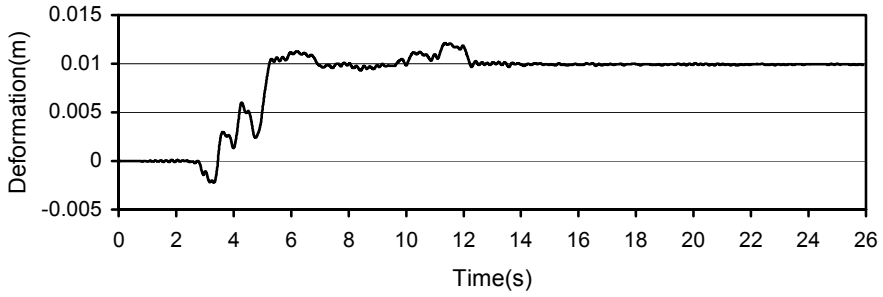

Figure 2.6 Deformation response of the inelastic system with $T_n = 0.2\,\text{sec}$ and $\xi = 0.05$ for $\bar{f} = 0.125$

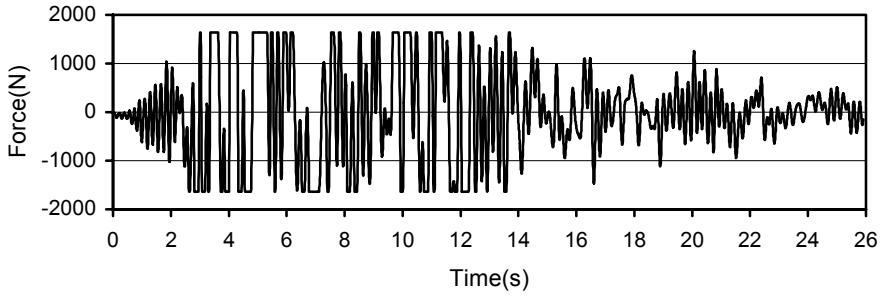

Figure 2.7 Resisting force response of the inelastic system with $T_n = 0.2\,\text{sec}$ and $\xi = 0.05$ for $\bar{f} = 0.125$

2.2.2.4 Inelastic response analysis of the system with $T_n = 5\,\text{sec}$

For the same system, the selected normalized yield strength $\bar{f} = 0.125$, the corresponding yield force $f_y = 203537.5N$ and the yield deformation $u_y = \dfrac{f_y}{k} = 0.0203537m$.

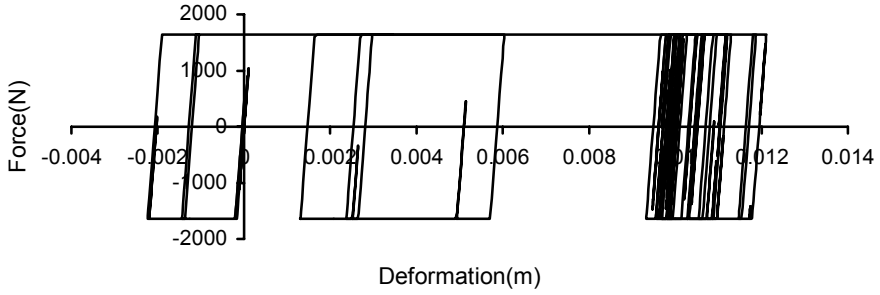

Figure 2.8 Force-deformation relation, hysterics loop, for the inelastic system with $T_n = 0.2\,\text{sec}$ and $\xi = 0.05$ for $\bar{f} = 0.125$

Initial calculations

$u_0 = 0$, $\dot{u}_0 = 0$, $p_0 = 0$

$$\ddot{u}_0 = \frac{p_0 - c\dot{u}_0 - k_0 u_0}{m} = 0 .$$

$\Delta t = 0.005$.

By the same C program through corresponding changes, inelastic deformation response, resisting force response and the force-deformation relation, hysterics loop, has been obtained and shown on Fig. 2.9, Fig. 2.10 and Fig. 2.11 respectively.

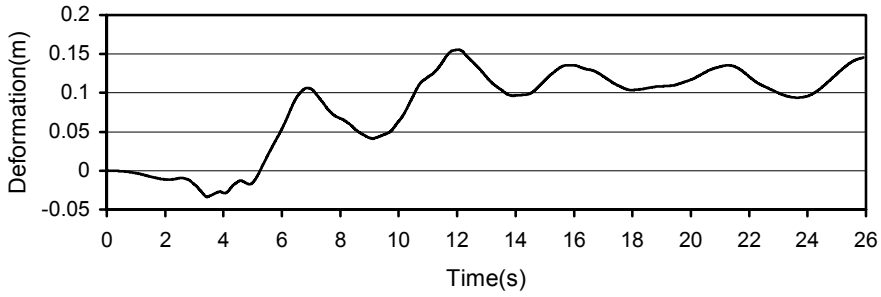

Figure 2.9 Deformation response of the inelastic system with $T_n = 5\,\text{sec}$ and $\xi = 0.05$ for $\bar{f} = 0.125$

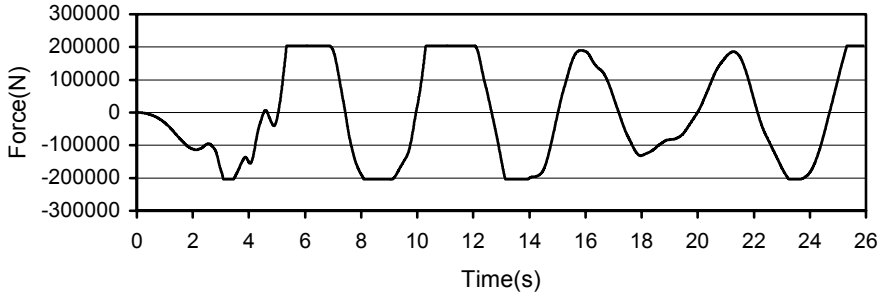

Figure 2.10 Resisting force response of the inelastic system with $T_n = 5\,\text{sec}$ and $\xi = 0.05$ for $\bar{f} = 0.125$

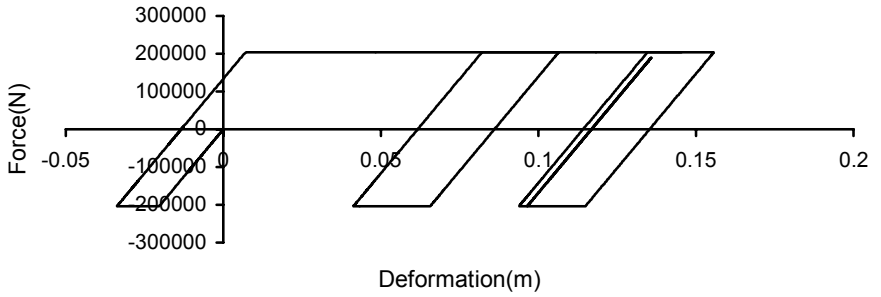

Figure 2.11 Force-deformation relation, hysterics loop, for the inelastic system with $T_n = 5\,\text{sec}$ and $\xi = 0.05$ for $\bar{f} = 0.125$

2.2.2.5 Numerical Calculation of Energy Quantities

The absolute energy and the relative energy terms of the given system have been evaluated separately by using the numerical results obtained from the preceding response analysis. Absolute input energy time histories for the systems with $T_n = 0.2\,\text{sec}$ and $T_n = 5\,\text{sec}$ are presented in Fig. 2.12, Fig. 2.13, and the separate plot of E_d, E_h, E_s, E_k time histories for them are shown at Appendix C and D respectively. Similarly, relative input energy time histories for the systems with $T_n = 0.2\,\text{sec}$ and $T_n = 5\,\text{sec}$ are presented in Fig. 2.14, Fig. 2.15, and the separate plot of E_d, E_h, E_s, E_k' time histories for them are shown at Appendix E and F respectively.

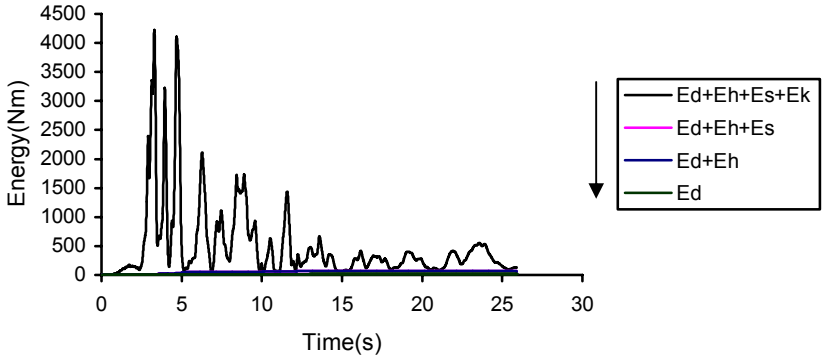

Figure 2.12 Absolute input energy time history of the system with $T_n = 0.2\,\text{sec}$ and $\xi = 0.05$ for $\bar{f} = 0.125$

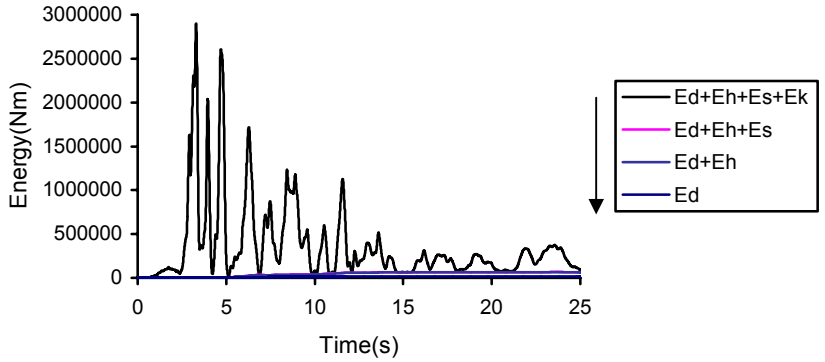

Figure 2.13 Absolute input energy time history of the system with $T_n = 5\,\text{sec}$ and $\xi = 0.05$ for $\bar{f} = 0.125$

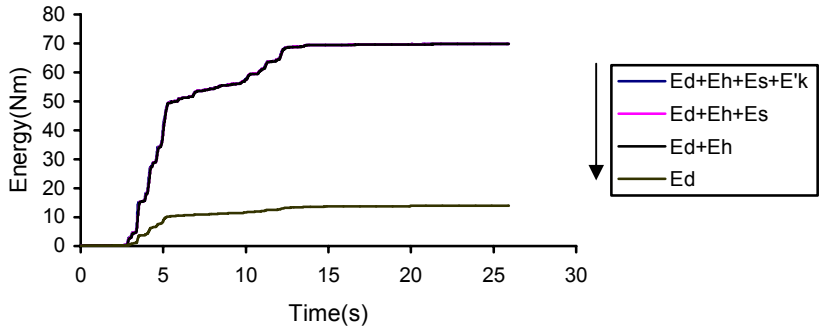

Figure 2.14 Relative input energy time history of the system with $T_n = 0.2\,\text{sec}$ and $\xi = 0.05$ for $\bar{f} = 0.125$

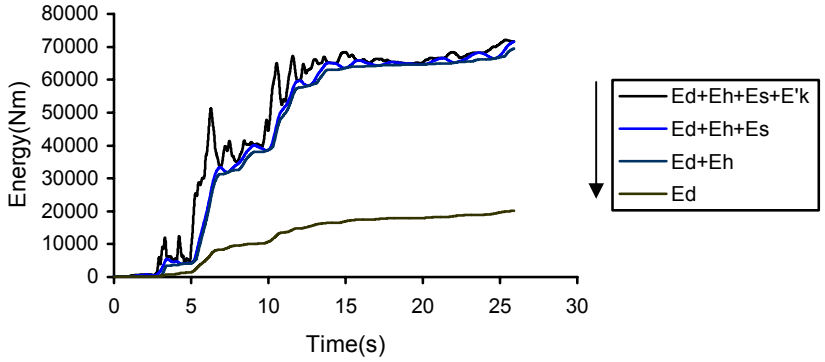

Figure 2.15 Relative input energy time history of the system with $T_n = 5\,\text{sec}$ and $\xi = 0.05$ for $\bar{f} = 0.125$

Similarly, relative input energy time history of the system with $T_n = 0.2\,\text{sec}$ and $\xi = 0.05$ for $\bar{f} = 0.25$ is presented in Fig. 2.16 in order to show the variation of energy depending on the normalized yield strength which reflects ductility of the structure. The value of energy decreases significantly when the ductility of the structure becomes low.

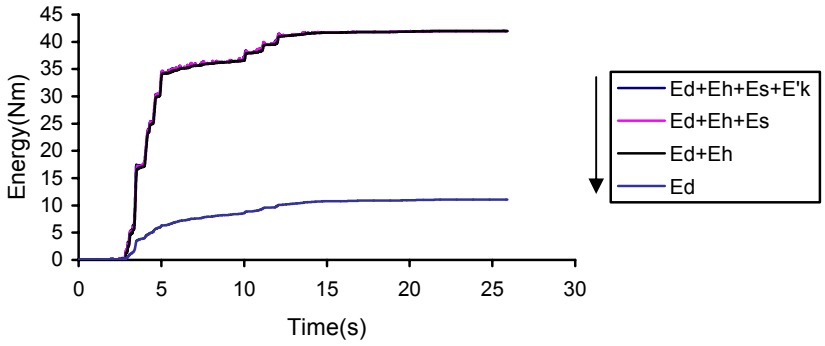

Figure 2.16 Relative input energy time history of the system with $T_n = 0.2\,\text{sec}$ and $\xi = 0.05$ for $\bar{f} = 0.25$

Input energy defined by either Eq. 2.9 or Eq. 2.13 is a function of time.

Damping energy E_d, strain energy E_s and hysteretic energy E_h are uniquely defined regardless of which formulation is used. However, the input energy and kinetic energy show difference regarding which method is used. The significant difference in magnitude of E_i and E_i' can be observed for the long period structure. The mass of the

structure almost does not move when the period of the structure is significantly larger than the predominant excitation period of the ground motion. Consequently, as it is explained in the E_i time history, the absolute input energy for the relatively long period structure should be low.

It is necessary to determine the time at which the input energy is evaluated in order to build input energy spectra. Mostly, the input energy is proposed to be evaluated at (i) the end of the ground motion duration, or (ii) this duration plus a time equal to one half the period of free vibration of the structure, or (iii) this duration plus a time at which the velocity of the structure changes sign. For short period structures, theses methods can generate proper results as far as the relative energy equation is used. However, for long period structures, they can significantly underestimate the maximum input energy that may occur early in the ground motion shaking.

2.3 Estimation of the Difference between Input Energies from Different Definitions

Both the absolute energy equation and the relative energy equation have been used by different authors depending on their purposes. The difference between the input energies defined by formulation 1 and formulation 2 can be calculated as

$$E_i = \int (m\ddot{u}_t)du_g = \int (m\ddot{u}_t)(du_t - du) = \int (m\ddot{u}_t)du_t - \int m(\ddot{u} + \ddot{u}_g)du$$
$$= \frac{m}{2}(\dot{u}_t)^2 - \frac{m}{2}(\dot{u})^2 + E_i' = \frac{m}{2}(\dot{u}_g)^2 + m\dot{u}\dot{u}_g + E_i'$$

so

$$E_i - E_i' = \frac{m}{2}(\dot{u}_g)^2 + m\dot{u}\dot{u}_g \qquad (2.3.1a)$$

The difference between the kinetic energies due to the different definitions also provides us the same result i.e.

$$E_k - E_k' = \frac{m}{2}(\dot{u}_g)^2 + m\dot{u}\dot{u}_g \,. \qquad (2.3.1b)$$

It is hard to evaluate the difference because of the term $\dot{u}$ in the last term of the previous equation. However, for the structures having very long and very short period, the value of E_i and E_i' are estimated below.

For a structure with very long period ($T \to \infty$), the input energy converges to a constant value depending on which definition of input energy is used. For a structure with infinitely long period,

$$u = -u_g$$

$$u_t = u + u_g = 0; \qquad \ddot{u}_t = 0$$

therefore,

Formulation 1: $$\frac{E_i}{m} = \int \ddot{u}_t du_g = \int (0) du_g = 0 \tag{2.3.2a}$$

Formulation 2: $$\frac{E_i'}{m} = -\int \ddot{u}_g du = -\int \ddot{u}_g (-du_g) = \int \ddot{u}_g (du_g) = \frac{(\dot{u}_g)^2}{2} \tag{2.3.2b}$$

i.e. the difference between the input energies E_i and E_i' for a structure $T \to \infty$ is equal to $\frac{m(\dot{u}_g)^2}{2}$. The value of the input energy E_i' evaluated at the end of duration will be very small because $\dot{u}_g$ tends to vanish gradually. If E_i' is evaluated as the maximum throughout the duration, $\frac{E_i'}{m}$ will converge to $\frac{u_{g(\max)}^2}{2}$ for structures with long period.

For a structure with very short period ($T \to 0$), the input energy also converges to a constant value depending on the different definitions. For a structure with zero period, i.e. a rigid structure,

$$\ddot{u}_t = \ddot{u}_g$$

$$u_t = u_g, \qquad u = 0,$$

therefore,

Formulation 1: $$\frac{E_i}{m} = \int \ddot{u}_t du_g = \int \ddot{u}_g du_g = \frac{(\dot{u}_g)^2}{2} \quad (2.3.3a)$$

Formulation 2: $$\frac{E_i'}{m} = -\int \ddot{u}_g du = -\int \ddot{u}_g(0) = 0 \quad (2.3.3b)$$

i.e. the difference between the input energies for a structure having zero period is $\frac{m\dot{u}_{g(\max)}^2}{2}$ [6].

2.4 The Relation between Energy-Based Velocity Spectrum and the Fourier Amplitude Spectrum

It is well known the energy-based velocity spectrum v_e of undamped elastic SDF systems is perfectly coincident with the Fourier amplitude spectrum, simply denoted by $|F(\omega)|$ [8]. The Fourier amplitude spectrum of base acceleration is defined by

$$|F(\omega)| = \left| \int_0^{t_0} \ddot{u}_g(t) e^{-i\omega t} dt \right| = \sqrt{\left(\int_0^{t_0} \ddot{u}_g(t) \cos \omega t dt \right)^2 + \left(\int_0^{t_0} \ddot{u}_g(t) \sin \omega t dt \right)^2} \quad (2.4.1)$$

As known, the kinetic energy of the mass is expressed as

$$E_k = \frac{1}{2} m[\dot{u}(t)]^2, \quad (2.4.2)$$

and the potential energy equal to the strain energy E_s is expressed as

$$E_s = \frac{1}{2} k[u(t)]^2 \quad (2.4.3)$$

The energy input consists of these two parts i.e.

$$E_i = \frac{1}{2} k[u(t)]^2 + \frac{1}{2} m[\dot{u}(t)]^2 \quad (2.4.5)$$

It is obvious that

$$\left(\frac{2E_i}{m}\right)^{\frac{1}{2}} = \left\{ [\omega_n u(t)]^2 + [\dot{u}(t)]^2 \right\}^{\frac{1}{2}} \tag{2.4.6}$$

where

$$\omega_n u(t) = \int_0^t \ddot{u}_g(\tau)\sin[\omega_n(t-\tau)]d\tau \tag{2.4.7}$$

$$\dot{u}(t) = \int_0^t \ddot{u}_g(\tau)\cos[\omega_n(t-\tau)]d\tau \tag{2.4.8}$$

Through substituting these expressions and some mathematical manipulations,

$$\sqrt{\frac{2E_i}{m}} = \left\{ \left[\int \ddot{u}_g(\tau)\cos\omega_n\tau d\tau\right]^2 + \left[\int \ddot{u}_g(\tau)\sin\omega_n\tau d\tau\right]^2 \right\}^{\frac{1}{2}}, \tag{2.4.9}$$

right hand side of which is the Fourier amplitude spectrum $|F(\omega)|$. If left hand side of Eq. 2.4.9 is denoted by the equivalent input energy velocity v_e,

$$|F(\omega)| = v_e \equiv \sqrt{\frac{2E_i}{m}} \tag{2.4.10}$$

2.5 Evaluation of Energy in Multi-Degree-of-Freedom-Systems

2.5.1 Energy Equations for the Original MDF Systems

2.5.1.1 Relative Energy Equation for MDF Systems

The governing equation of motion for a MDF system is given by

$$[m]\{\ddot{u}\} + [c]\{\dot{u}\} + \{f_s(\{u\})\} = -[m]\{1\}\ddot{u}_g \tag{2.5.1}$$

where $[m]$, $[c]$, $\{f_s(\{u\})\}$ and $\{u\}$ are the diagonal mass matrix, viscous damping matrix, restoring force vector and relative displacement vector respectively [9].

Integrating Eq. 2.5.1 in the displacement range, we get

$$\int [m]\{\ddot{u}\}\{du\}^T + \int [c]\{\dot{u}\}\{du\}^T + \int \{f_s(\{u\})\}\{du\}^T = -\int [m]\{1\}\ddot{u}_g\{du\}^T \tag{2.5.2a}$$

Considering $\{du\}^T = \{\dot{u}\}^T dt$, we can rewrite Eq. 2.5.2a with respect to time as

$$\int \{\dot{u}\}^T [m]\{\ddot{u}\}dt + \int \{\dot{u}\}^T [c]\{\dot{u}\}dt + \int \{\dot{u}\}^T \{f_s(\{u\})\}dt = -\int \{\dot{u}\}^T [m]\{1\}\ddot{u}_g dt \quad (2.5.2b)$$

The first term is the kinetic energy E_k, the second term is the damping energy E_d, the third term is the sum of the irrecoverable hysteretic energy E_h and the recoverable elastic strain energy E_s. The right hand side term is the input energy E_i.

For the purpose of comparison among different systems, it is useful to normalize the various energy terms to the total mass of the system.

2.5.1.2 Absolute Energy Equation for MDF Systems

The absolute energy equation for multi-degree-of-freedom-systems subjected to an earthquake excitation has been derived as below:

$$\frac{1}{2}\{\dot{u}_t\}^T [m]\{\dot{u}_t\} + \int \{\dot{u}\}^T [c]d\{u\} + \int \{f_s\}^T d\{u\} = \int (\sum_{i=1}^{n} m_i \ddot{u}_{ti})du_g \quad (2.5.3)$$

where $\ddot{u}_{ti}$ is the absolute acceleration at the ith floor. The kinetic energy and input energy are obtained as below.

$$E_k = \frac{1}{2}\{\dot{u}_t\}^T [m]\{\dot{u}_t\} = \frac{1}{2}\sum_{i=1}^{n} m_i (\dot{u}_{ti})^2 \quad (2.5.4a)$$

$$E_i = \int (\sum_{i=1}^{n} m_i \ddot{u}_{ti})du_g \quad (2.5.4b)$$

where E_k is the summation of the kinetic energy at each floor level due to an absolute velocity $\dot{u}_{ti}$ at the ith floor, and E_i is the summation of the work done by an inertia force $m_i \ddot{u}_{ti}$ at each floor for ground displacement [6].

2.5.2 Energy Equations for the Equivalent SDF Systems

2.5.2.1 Seismic Analysis of a MDF System Using SDF Equivalent System

A simplified approach for the seismic analysis of a MDF system using the seismic response of the corresponding equivalent SDF system has been presented here using the dimensional form of the equations of motion [8]. Firstly, the multistory building is assumed to have a constant deflection shape $\{\phi\}$. Hence the relative displacement vector $\{u(t)\}$ can be written as

$$\{u(t)\} = \{\phi\}\delta(t) \tag{2.5.5}$$

where $\delta(t)$ is the lateral displacement at the roof level.

Substituting Eq. 2.5.5 into the equation of motion of the building subjected to an earthquake ground motion, we get

$$\ddot{\delta}(t) + 2\xi\omega^*\dot{\delta}(t) + \frac{R^*(t)}{M^*} = -\gamma\ddot{u}_g(t) \tag{2.5.6}$$

where ω^* is the fundamental circular frequency of the building, and

$$M^* = \{\phi\}^T[m]\{\phi\} \tag{2.5.7}$$

$$R^*(t) = \{\phi\}^T\{R(t)\} \tag{2.5.8}$$

$$\gamma = \frac{L^*}{M^*} \tag{2.5.9}$$

$$L^* = \{\phi\}^T[m]\{1\} \tag{2.5.10}$$

where $[m]$ is a diagonal mass matrix and $\{R(t)\}$ is the resistance vector with terms associated with each lateral degree of freedom.

Solution of Eq. 2.5.6 in the range $\delta \le \delta_y$

Let's remind the equation of motion of SDF system:

$$\ddot{u}(t) + 2\xi\omega\dot{u}(t) + \frac{f_s(t)}{m} = -\ddot{u}_g(t) \tag{2.5.11}$$

The restoring force terms of Eq. 2.5.6 and Eq. 2.5.11 can be written respectively as

$$\frac{R^*(t)}{M^*} = \omega^{*2}\delta(t) \tag{2.5.12}$$

$$\frac{f_s(t)}{m} = \omega^2 u(t) \tag{2.5.13}$$

Substituting Eq. 2.5.12 into Eq. 2.5.6 leads to

$$\ddot{\delta}(t) + 2\xi\omega^*\dot{\delta}(t) + \omega^{*2}\delta(t) = -\gamma\ddot{u}_g(t) \tag{2.5.14}$$

Comparison of Eq. 2.5.14 and the combination of Eq. 2.5.13 and Eq. 2.5.11 shows that when $\omega = \omega^*$, if $u(t)$ is the solution of Eq. 2.5.11, $\gamma u(t)$ would be the solution of Eq. 2.5.14. That is

$$\delta(t) = \gamma u(t) \tag{2.5.15}$$

From Eq. 2.5.15, we can write

$$\delta_y = \gamma u_y \tag{2.5.16}$$

Combining Eq. 2.5.12, Eq. 2.5.13 and Eq. 2.5.15, we can write

$$\frac{R^*(t)}{M^*} = \gamma\frac{f_s(t)}{m} \tag{2.5.17}$$

Solution of Eq. 2.5.6 in the inelastic range

For solving Eq. 2.5.6 in the inelastic range, it is assumed that the global displacement ductility ratio of the building and the displacement ductility ratio of the SDF system are equal, i.e.

$$\frac{\delta(t)}{\delta_y} = \frac{u(t)}{u_y} \tag{2.5.18}$$

Eq. 2.5.15 can also be obtained by combining Eq. 2.5.16 and Eq. 2.5.18. Therefore, if $u(t)$ is the solution of the nonlinear Eq. 2.5.11, $\gamma u(t)$ would be the solution of Eq. 2.5.6 in the inelastic range.

Substituting Eq. 2.5.17 into Eq. 2.5.6, we can get

$$\ddot{\delta}(t) + 2\xi\omega^* \dot{\delta}(t) + \gamma \frac{f_s(t)}{m} = -\gamma \ddot{u}_g(t) \tag{2.5.19}$$

Inspection of the above equation and Eq. 2.5.11 shows that the solution of the equation of motion of the equivalent nonlinear SDF system is given by Eq. 2.5.15, which proves that Eq. 2.5.17 is also valid for the inelastic range.

2.5.2.2 Energy Equations for the Equivalent SDF Systems

Integration of the differential equation of motion of the equivalent SDF system, Eq. 2.5.19, with respect to δ leads to

$$\int \ddot{\delta}(t)d\delta + 2\xi\omega^* \int \dot{\delta}(t)d\delta + \int \gamma \frac{f_s(t)}{m} d\delta = -\int \gamma \ddot{u}_g(t)d\delta \tag{2.5.20}$$

Substituting Eq. 2.5.15 into Eq. 2.5.20, we can get

$$\gamma^2 \int \ddot{u}(t)du + 2\xi\omega^* \gamma^2 \int \dot{u}(t)du + \gamma^2 \int \frac{f_s(t)}{m} du = -\gamma^2 \int \ddot{u}_g(t)du \tag{2.5.21}$$

The third term on the left hand side of the above equation represents the hysteretic energy E_h^* plus the strain energy E_s^* of the equivalent SDF system, i.e.

$$E_h^* + E_s^* = \gamma^2 \int \frac{f_s(t)}{m} du \tag{2.5.22}$$

As known, for a SDF system, the sum of hysteretic energy per unit mass plus the elastic strain energy per unit mass is given by

$$E_h + E_s = \int \frac{f_s(t)}{m} du \tag{2.5.23}$$

Combining Eq. 2.5.23 and Eq. 2.5.22 yields

$$E_h^* + E_s^* = \gamma^2 (E_h + E_s) \tag{2.5.24}$$

Using the definition of hysteretic energy, from Eq. 2.5.24 we can write

$$E_h^* = \gamma^2 E_h \tag{2.5.25}$$

PART 3 STATISTICAL EVALUATION OF ENERGY IN STRUCTURES

It is very cumbersome to calculate the energy quantities by the analytical method presented in the previous part. In order to eliminate this difficulty, many statistical approaches for the evaluation of energy components, especially input energy which is a key parameter in the seismic assessment of structures and earthquakes, have been proposed by researchers. In this part, two of them proposed by Fajfar [9] and Manfredi [4] have been introduced respectively.

3.1 A Procedure for Estimating Input Energy Spectra

3.1.1 Introduction

The potential for accumulation of damage that may occur in the structure subjected to an earthquake with long duration and large magnitude is an important issue in seismic design of structures. As far as the long-duration ground motions are concerned, yielding structures experience an increased number of cycles into the inelastic range; the concerning damage may significantly influence the whole performance of the structure depending on the damage characteristics of the structure. Formulation of duration-dependent inelastic seismic design spectra was developed by Fajfar and his colleagues. This approach uses the suggestion which assumes that the lateral strength of a structure can be increased to compensate for the cumulative damage associated with an increased duration of the ground motion. The estimation of seismic demand in the form of an input energy spectrum forms the main procedure in the formulation of duration-dependent seismic design spectra. In the recent approach, the input energy is estimated by making use of the ground motion parameters which include the duration of the ground motion. An inelastic seismic design spectrum is developed by requiring that the structure has cyclic plastic strain energy capacity that is larger than or equal to the portion of the

seismic input energy contributing to cumulative damage. The plastic strain energy capacity is determined using an energy-based cumulative damage model.

3.1.2 Equivalent Input Energy Velocity Spectrum

3.1.2.1 Basic equations

In seismic design of structures, the damage potential of an earthquake ground motion can be evaluated in terms of the total power associated with the acceleration of the ground motion. The total power of an earthquake ground motion can be evaluated by the similar procedure to the evaluation of the total power of a random signal. Particularly, the well-known Parseval's theorem proposes that the total power associated with an earthquake ground acceleration $\ddot{u}_g(t)$ can be computed by an integral either in the time domain or the frequency domain i.e.

$$\text{Total Power} = \int_{-\infty}^{\infty} \ddot{u}_g(t)^2 dt = \frac{1}{2\pi} \int_{-\infty}^{\infty} \left|F(\omega)\right|^2 d\omega \tag{3.1.1}$$

where ω=circular frequency, and $\left|F(\omega)\right|$=Fourier amplitude spectrum of the ground acceleration $\ddot{u}_g(t)$. The Fourier transform of the ground acceleration $\ddot{u}_g(t)$ is expressed as:

$$F(\omega) = \int_{-\infty}^{\infty} \ddot{u}_g(t) e^{-i\omega t} dt \tag{3.1.2}$$

where $i = \sqrt{-1}$. Because the ground acceleration involves only a real function, the below property is true for the Fourier transform of the ground acceleration:

$$F(-\omega) = F(\omega)^* \tag{3.1.3}$$

where $F(\omega)^*$ is the complex conjugate of the Fourier transform of the ground acceleration. Using the special property in Eq. 3.1.3, and replacing the limits of the integration in the time domain by $t = 0$ and $t = t_0$ where t_0 is the length of the digitized ground accelerogram, and the limits of integration in the frequency domain by $\omega = 0$ to $\omega = \infty$, Eq. 3.1.1 can be written as:

$$\int_0^{t_0} \ddot{u}_g(t)^2 dt = \frac{1}{\pi}\int_0^{\infty} |F(\omega)|^2 d\omega . \tag{3.1.4}$$

The left hand side of Eq. 3.1.4 can also be written as the mean square of the ground acceleration $\sigma_{\ddot{u}_g}{}^2$ times the length of the digitized accelerogram t_0. Thus the total power of the ground acceleration can be written as:

$$\text{Total Power} = \sigma_{\ddot{u}_g}{}^2 t_0 = \frac{1}{\pi}\int_0^{\infty} |F(\omega)|^2 d\omega . \tag{3.1.5}$$

However, the peak-ground-acceleration $(\ddot{u}_g)_{\max}$ is more often used to define the intensity of the ground motion rather than the root-mean-square (RMS) of the ground acceleration $\sigma_{\ddot{u}_g}$ for seismic design of structures. Therefore, the root-mean-square of the ground acceleration $\sigma_{\ddot{u}_g}$ is expressed in terms of the peak-ground-acceleration $(\ddot{u}_g)_{\max}$ using a peak factor Z which estimates the most probable peak-ground-acceleration for a given RMS value of the ground acceleration, i.e.

$$(\ddot{u}_g)_{\max} \equiv Z\sigma_{\ddot{u}_g} . \tag{3.1.6}$$

RMS of the ground acceleration can be expressed as $\sigma_{\ddot{u}_g} = \sqrt{\frac{1}{n}\sum_{i=1}^{n}\left[\ddot{u}_g(t_i)\right]^2}$.

Using the above definition for the peak factor Z, Eq. 3.1.5 can be written as:

$$\left(\frac{(\ddot{u}_g)_{\max}}{Z}\right)^2 t_0 = \frac{1}{\pi}\int_0^{\infty} |F(\omega)|^2 d\omega . \tag{3.1.7}$$

The peak factor Z will be discussed later.

It is necessary that the integral on the right hand side of Eq. 3.1.7 be evaluated in order to build the equivalent input energy velocity spectrum. However, the Fourier amplitude spectrum of the ground acceleration $|F(\omega)|$ is highly variable and makes it hard to carry out the integration directly. However, it is worth noting that the Fourier amplitude spectrum of ground acceleration $|F(\omega)|$ is identical to the equivalent input energy velocity v_e for an elastic, undamped SDF system, i.e.

$$\left|F(\omega)\right| = v_e \equiv \sqrt{\frac{2E_i}{m}} \tag{3.1.8}$$

It has been shown that the presence of damping in the structure tends to smooth out the irregular peaks in the input energy spectrum without significantly affecting the average value of the spectrum. Based on the numerical analyses of inelastic structural response under earthquake excitations, it has been concluded that the input energy at the end of the ground motion is not very sensitive to the lateral strength of the structure. Therefore, Eq. 3.1.8 can be considered to provide a good estimation of the input energy to structures.

Due to the observation that the maximum input energy per unit mass approaches $\frac{(\dot{u}_g)^2_{\max}}{2}$ as the period of the structure $T \to \infty$ where $(\dot{u}_g)_{\max}$ is the peak-ground-velocity, the equivalent input energy velocity v_e can be written as a product of an amplification factor Ω_v and the peak-ground-velocity $(\dot{u}_g)_{\max}$, i.e.

$$v_e = \Omega_v (\dot{u}_g)_{\max} \tag{3.1.9}$$

where the amplification factor Ω_v depends on the ground motion parameters and the period of the structure. This approach is commonly used in energy-based seismic design of structures. The equivalent input energy velocity spectrum can be defined in terms of the amplification factor Ω_v using this approach. Relating to the input energy to a structure, it is necessary to note that the maximum input energy and the input energy calculated at the end of the ground motion is not identical. At very long period $T \to \infty$, the maximum input energy does not occur at the end of the ground motion but occurs well before the end of the ground motion. A large portion of the maximum input energy is stored as the kinetic energy and elastic strain energy and do not contribute to the cumulative damage of the structure although the maximum input energy per unit mass approaches $\frac{(\dot{u}_g)^2_{\max}}{2}$ when $T \to \infty$. The use of input energy at the end of the ground motion which includes the energy dissipated by all inelastic cycles, rather than the maximum input energy, is more proper when the effect of cumulative damage is taken

into account in seismic designing. The input energy calculated at the end of the ground motion, and hence the amplification factor Ω_v, should therefore tend to zero when the period $T \to \infty$.

3.1.2.2 Spectral Shape and Peak Amplification Factor

According to the studies of inelastic dynamic response of SDF systems, for a given lateral strength of the system, a general shape shown in Fig. 3.1 can be adopted for the amplification factor Ω_v characterizing the input energy at the end of the ground motion. The peak amplification factor Ω_v^* occurs at the characteristic period T_c of the ground motion. The characteristic period T_c will be discussed further later in this study. Defining the spectral shape in Fig. 3.1 in detail, the amplification factor Ω_v is assumed to tend to zero when the period $T \to 0$, and when $T \to \infty$. In this study, below spectrum is adopted for the amplification factor:

$$\Omega_v = \begin{cases} \Omega_v^* \left[\dfrac{T}{T_c} \right] & if\ 0 \le T \le T_c \\ \Omega_v^* \left[\dfrac{T}{T_c} \right]^{-\lambda} & if\ T_c < T < \infty \end{cases} \tag{3.1.10}$$

where Ω_v^*=peak amplification factor for the equivalent input energy velocity, and $\lambda \ge 0$, where λ defines the spectral shape for period larger than the characteristic period. A value of $\lambda = 0$ defines a bilinear spectrum whereas a large value of λ defines a spectral shape having faster rate of decrease for the amplification factor Ω_v in the long period range. The proposed spectral shape for Ω_v enables us to integrate the right hand side of Eq. 3.1.7 to obtain:

$$\frac{1}{\pi} \int_0^\infty |F(\omega)|^2 d\omega = \frac{2(\ddot{u}_g)_{\max}^2 (\Omega_v^*)^2}{T_c} \left(\frac{2\lambda + 2}{2\lambda + 1} \right) \tag{3.1.11}$$

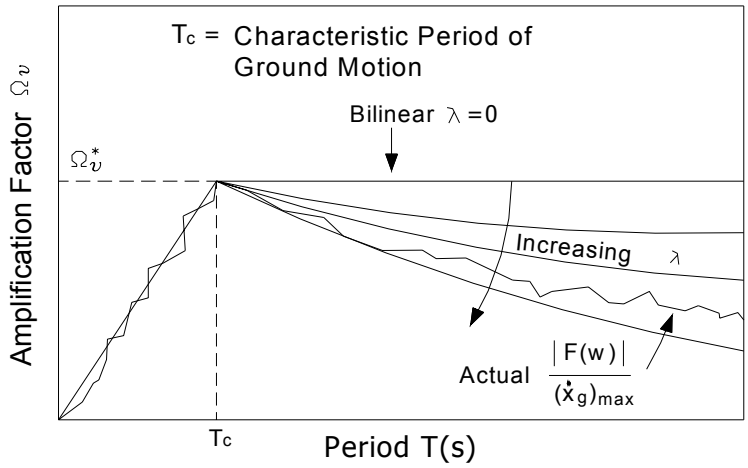

Figure 3.1 Amplification factor Ω_v for equivalent input energy velocity

In the damage assessment of structures subjected to earthquake ground motions, the duration corresponds to the strong motion phase of the ground motion t_d is more important than the length of the digitized accelerogram t_0. Consequently, it is more proper to replace the length of digitized accelerogram t_0 in Eq. 3.1.7 by the strong motion duration t_d when the total power of the ground acceleration is calculated. However, it is necessary to conduct a proper adjustment of the peak factor Z when performing the replacement. This will be discussed later on. Although various definitions have been proposed for the duration of strong ground motion, the definition by Trifunac and Brady will be used here:

$$t_d = t_{0.95} - t_{0.05} \tag{3.1.12}$$

where $t_{0.05}$ and $t_{0.95}$ correspond to the times when 5% and 95% of the final Arias intensity are reached by the ground motion. Replacing t_0 by t_d, Eq. 3.1.7 and Eq. 2.1.11 can be combined to give the peak amplification factor Ω_v^* for the equivalent input energy velocity:

$$\Omega_v^* = \frac{(\ddot{u}_g)_{\max}}{Z(\dot{u}_g)_{\max}} \sqrt{t_d T_c} \sqrt{\frac{\lambda + 1/2}{2\lambda + 2}} \qquad \text{where} \quad \lambda \geq 0 \tag{3.1.13}$$

where the peak amplification factor Ω_v^* for the equivalent input energy velocity is now expressed in terms of the ground motion parameters $(\dot{u}_g)_{\max}$, $(\ddot{u}_g)_{\max}$, t_d, T_c and the peak factor Z. The peak amplification factor defined by Eq. 3.1.13 is not significantly dependent on the variation of λ for large value of λ (say $\lambda \geq 1$). Depending on the variation of λ from 1 to 2, the peak amplification factor decreases by about 5%. A value of $\lambda = 1$ is used unless otherwise stated for discussion results later in this study. It can also be seen from the resulting expression, Eq. 3.1.13 that the peak amplification factor Ω_v^* is only dependent on the square root of the characteristic period T_c, although is supposed to occur at the characteristic period T_c. The peak amplification factor Ω_v^*, which is a key parameter for the spectrum, is not significantly dependent on where the exact period occurs.

3.1.2.3 Peak-to-RMS Ratio for Ground Acceleration

Presenting the equivalent input energy velocity spectrum requires that the peak factor Z representing the ratio between peak-ground-acceleration and root-mean-square of the ground acceleration be estimated. However, for a nonstationary process, it is generally difficult to estimate the peak factor. In estimating the peak factor Z, one of the various expressions proposed in the literature based on the assumption of a stationary process, which has been resulted from a study of wind effects on structures, is presented here:

$$Z = \sqrt{2\ln\left(\omega \frac{t_{d1}}{2\pi}\right)} + \frac{\gamma}{\sqrt{2\ln\left(\omega \frac{t_{d1}}{2\pi}\right)}} \tag{3.1.14}$$

where γ=Euler constant=0.577, ω=circular frequency of the system, and t_{d1} corresponds to a segment of the stationary excitation where the peak factor is to be determined, and t_{d1} is usually used to express some measure of the "duration" of the ground motion when the expression is presented for earthquake excitation. A different expression for the peak factor has also been proposed for the vibration analysis of structures under random seismic excitation assumed to have a stationary process:

$$Z = \sqrt{2\ln\left[-\frac{\omega}{\pi}\frac{t_{d2}}{\ln(1-p)}\right]} \tag{3.1.15}$$

where p =probability of exceedance, and t_{d2} represents a measure of the "duration" of the excitation and has identical meaning as t_{d1}. For a probability of exceedance in the range of $0.1 \le p \le 0.3$, the peak factors obtained from Eq. 3.1.14 and Eq. 3.1.15 are very close to each other, and are not very sensitive to the duration t_{d1} or t_{d2}, nor the circular frequency ω of the structure. Consequently, a constant value for the peak factor $Z = 3$ has been suggested for use.

It is not proper to use the direct values of the peak factors obtained from Eq. 3.1.14 or Eq. 3.1.15, or a constant value of $Z = 3$ for the estimation of the peak amplification factor Ω_v^*, because the term t_d in Eq. 3.1.13 has been defined based on the definition of the strong motion duration proposed by Trifunac and Brady. However, the appropriate value of the peak factor can be estimated through the statistical study of the peak factor using ground motion records. By rewriting Eq. 3.1.4-Eq. 3.1.6, the peak factor can be expressed as:

$$Z \equiv \sqrt{\frac{(\ddot{u}_g)^2_{\max} t_d}{\int_0^{t_0} \ddot{u}_g(t)^2 dt}}\,. \tag{3.1.16}$$

In estimating the peak factor Z, a statistical study has been conducted by Fajfar evaluating Eq. 3.1.16 using 118 ground motions recorded in California. Even though the set of data points tend to be concentrated in the short duration rage ($t_d < 20$ sec), the peak factor varies primarily between 2 and 6, and seems to be insensitive to the duration of the ground motion, as noted earlier for Eq. 3.1.14 and Eq. 3.1.15. The mean value of the peak factor is obtained as $\overline{Z} = 3.98$, and the standard deviation is $\sigma_z = 0.81$. Consequently, a constant peak factor of $Z = 4$ is suggested to be used for the estimation for the peak amplification factor Ω_v^* in accordance with t_d defined by Eq. 3.1.12 for the strong ground motion duration.

3.1.3 Characteristic Periods of Ground Motions

The use of input energy spectrum requires an estimation of the characteristic period T_c, which represents the period at which the peak value of the input energy occurs. In the literature, this period may be called either the characteristic period or predominant period of the ground motion. The former will be used in this study. However, a given ground motion does not have a unique characteristic period since it is dependent on the lateral strength of the system, to a lesser extent, on the damping of the system. The assumption accepted for the approach proposed in this study is that the characteristic period corresponds to the transition period between the acceleration-controlled and velocity controlled elastic response spectrum, and may be defined by:

$$T_c = 2\pi \frac{c_v}{c_a} \frac{(\dot{u}_g)_{\max}}{(\ddot{u}_g)_{\max}} \tag{3.1.17}$$

where c_v corresponds to the ratio of the spectral elastic response velocity to peak-ground-velocity in the velocity-controlled (medium) period range, and c_a corresponds to the ratio of the spectral elastic response acceleration to peak-ground-acceleration in the acceleration-controlled (short) period range. The coefficients c_v and c_a have been taken as 2.0 and 2.5 respectively in the duration-dependent inelastic seismic design spectra.

3.1.4 Comparison of Peak Amplification Factors Ω_v^*

3.1.4.1 Comparison with Ground Motions

Using a peak factor of $Z = 4$, and a value of $\lambda = 1$, and substituting the characteristic period T_c as given by Eq. 3.1.1 into Eq. 3.1.13 with coefficients $c_v = 2$ and $c_a = 2.5$, the expression for the peak amplification factor Ω_v^* reduces to:

$$\Omega_v^* = 0.343 \sqrt{\frac{(\ddot{u}_g)_{\max} t_d}{(\dot{u}_g)_{\max}}} \,. \tag{3.1.18}$$

Eq. 3.1.18 indicates that the peak amplification factor Ω_v^* is proportional to the square root of the a/v ratio and the strong motion duration t_d of the ground motion.

3.1.4.2 Comparison with Peak Amplification Factor Obtained from Bilinear Equivalent Input Energy Velocity Spectrum

A bilinear spectrum was proposed by Kuwamura and Galambos for the equivalent input energy velocity. In this study, the peak equivalent input energy velocity v_{eo} is given by:

$$v_{eo} = \frac{1}{2}\sqrt{T_c \int_0^{t_0} \ddot{u}_g(t)^2 dt} \tag{3.1.19}$$

where T_c may be taken as the characteristic period of the ground motion, $\ddot{u}_g(t)$=ground acceleration time history, and $t_0 =$ length of digitized accelerogram. By replacing the peak equivalent input energy velocity by the product of the peak amplification factor and the peak-ground-velocity i.e. $v_{eo} = \Omega_v^*(\dot{u}_g)_{\max}$, and the integral of the square of the ground acceleration by:

$$\int_0^{t_0} \ddot{u}_g(t)^2 dt = \left(\frac{(\ddot{u}_g)_{\max}}{Z}\right)^2 t_d \tag{3.1.20}$$

where the length of the digitized accelerogram t_0 has been replaced by the strong motion duration t_d, and the peak factor Z has been defined in conjunction with the strong motion duration t_d, the below peak amplification factor for the equivalent input energy velocity can be obtained from Eq. 3.1.19: i.e.

$$(\Omega_v^*)_{bl} = \frac{(\ddot{u}_g)_{\max}}{2Z(\dot{u}_g)_{\max}}\sqrt{t_d T_c}\ . \tag{3.1.21}$$

It is worth noting that the peak amplification factor defined by Eq. 3.1.21 is similar with that obtained from Eq. 3.1.13 for the value of $\lambda = 0$ for the bilinear equivalent input energy velocity spectrum. By the way, it should be noted that a bilinear spectrum underestimates the peak amplification factor. Therefore, the value of the peak amplification factor defined by Eq. 3.1.19 for a bilinear spectrum was suggested to be

increased by 27%. It is also observed that the peak amplification factor resulted from Eq. 3.1.13 with the replacement of $\lambda = 1$ is 22% larger that that obtained from Eq. 3.1.21 for a bilinear spectrum.

3.1.4.3 Comparison with Empirical Formula

In a study by Vidic and Fajfar, an empirical formulation was proposed to estimate the peak amplification factor i.e.

$$(\Omega_v^*)_{emp} = 0.69\left(\frac{(\ddot{u}_g)_{\max} t_d}{(\dot{u}_g)_{\max}}\right)^{3/8} . \tag{3.1.22}$$

In comparing the peak amplification factors obtained from Eq. 3.1.18 with that obtained from Eq. 3.1.22, the peak amplification factors estimated by the two equations are highly identical to each other for the duration range $10 \le t_d \le 55$ sec. However, for a short duration range e.g. $t_d < 10$ sec, the empirical peak amplification factor $(\Omega_v^*)_{emp}$ can be significantly larger than that predicted by the formula, especially for low a/v ratio. Contrarily, the peak amplification factor predicted by the empirical expression Eq. 3.1.22 is slightly smaller than that predicted by the formula Eq. 3.1.18 for a long duration e.g. $t_d > 20$ sec and for high and ultrahigh a/v ratios. To sum up, the variation of the peak amplification factor in accordance with strong motion duration t_d and a/v ratio can be seen as the major difference between the two peak amplification factors. In considering the empirical expression Eq. 3.1.22, the peak amplification factor varies depending on duration and a/v ratio as a power of 3/8, while the peak amplification factor obtained from Eq. 3.1.18 varies as a square root of the duration and a/v ratio.

3.2 Evaluation of Seismic Energy Demand

3.2.1 Hysteretic Energy and Equivalent Number of Cycles

The amount of the hysteretic energy E_h definitely influences the cyclic collapse of structures with a degrading behavior. This provides us the possibility to define a damage functional based on the assumption that the structural collapse occurs when the

hysteretic energy dissipated under seismic actions is equal to the energy dissipated under monotonic load. We can evaluate the allowable hysteretic energy via a theoretical or experimental analysis of monotonic tests. If the allowable plastic energy of the structure analyzed is denoted with $E_{h,u}$, the seismic check can be represented as below:

$$E_h \leq E_{h,u} \tag{3.2.1}$$

As mentioned, the energy criterion has the limitation which requires that all the plastic cycles be taken into account adding the dissipated energy regardless of the amplitude of each cycle. Therefore, a measure of the distribution of cycles amplitude is the equivalent number of cycles n_{eq} which represents the number of cycles at the maximum plastic displacement that the structure can undergo in order to dissipate the total amount of the hysteretic energy E_h:

$$E_h = n_{eq} F_y (u_{\max} - u_y) \tag{3.2.2a}$$

$$n_{eq} = \frac{E_h}{F_y (u_{\max} - u_y)} \tag{3.2.2b}$$

where E_h is the total dissipated energy, F_y is the maximum force of the structure, $u_{\max}$ is the maximum displacement and u_y is the displacement at the elastic limit.

Furthermore, in order to characterize the non-linear behavior of a SDF system, the reduction factor R can be represented referring to the elastic spectral acceleration $S_a(T)$ as

$$R = \frac{mS_a(T)}{F_y} = \frac{1}{\mu} \tag{3.2.3}$$

where m is the mass of the structure.

The values of n_{eq} close to 1 indicate that the nonlinear system undergoes a large plastic cycle whereas the high values of n_{eq} indicate many plastic cycles there are in the response. Several analysis of n_{eq} versus the elastic period T of the system for various

reduction factor R and different earthquakes show that n_{eq} generally decreases with the period in the short period range and increases with the reduction factor.

Furthermore, it is also observed that the values of n_{eq} are extensively sensitive to the earthquake characteristics. Its values vary from 1 for impulsive earthquakes to nearly 40 for long-duration earthquakes. This means that there is high correlation between the values of n_{eq} and the characteristics of the earthquake.

3.2.2 The Assessment of the Equivalent Number of Cycles

The number of reversal plastic cycles n with an amplitude of the generic cycle equal to Δu_i, maximum amplitude $\Delta u_{\max}$ and the dimensionless average amplitude of the $n-1$ cycles cutting of the plastic cycle of maximum amplitude

$$x = \frac{1}{(n-1)} \sum_{i=1}^{n-1} \frac{\Delta u_i}{\Delta u_{\max}}$$

can represent the nonlinear response of an elastoplastic SDF system under an earthquake ground motion.

This results in a different expression of the number of equivalent cycles i.e.

$$n_{eq} = 1 + (n-1)x \,. \tag{3.2.4}$$

Consequently, it is noted that the evaluation of n and x defines n_{eq}.

Fig. 3.2 illustrates the typical calculation of these quantities.

An extensive statistical analysis has been conducted in order to define n and x reliably. The procedure of the analysis has been implemented in the analytical formulations performing the following steps:

(1) a set of possible structural (i.e. stiffness, yielding level, damping, etc.) and earthquake (i.e. peak ground acceleration (PGA), peak ground velocity (PGV), duration, etc.) parameters, correlated with n and x, has been introduced;

(2) an exponential type formulation has been selected for n and x:

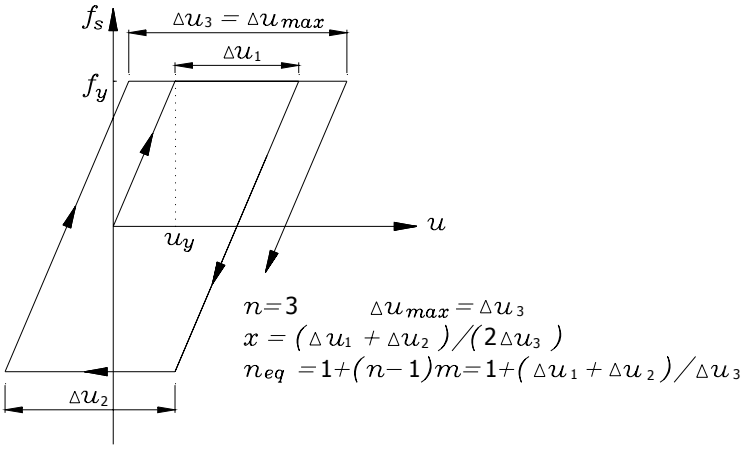

Figure 3.2 Calculation of n and x

$$n = 1 + A p_{e,i}^{\alpha} p_{p,i}^{\beta} p_{s,i}^{\gamma} \qquad x = 1 + B p_{e,i}^{\delta} p_{p,i}^{\varepsilon} p_{s,i}^{\lambda}$$

where p_e, p_p and p_s are the possible earthquake and structural parameters;

(3) statistical regression was performed comparing the values of n and x, obtained from a nonlinear step by step integration of SDF equation, and the values provided by the proposed formulations;

(4) the optimum parameters were defined choosing the parameters with the higher partial correlation factor;

(5) the optimum coefficients A, B, α, β, γ, δ, ε and λ were chosen minimizing the standard error.

Afterwards, as for the structural parameters, the relations by the ratio $\delta = \xi / \xi_0$, where ξ is the proportional damping and ξ_0 is 5% reference damping, and the ratio $\tau = T / T_1$ (for $T < T_1$), where T is the elastic period of the system and T_1 is the initial period of the medium periods range in the Newmark and Hall spectral representation, describes the elastic response while $(R-1)$, where R is the reduction factor, describes the inelastic response.

A fundamental procedure, the assessment of the seismic characteristics necessary for the identification of n and x are performed using following parameters, functions and indices. A dimensionless index I_D

$$I_D = \frac{I_E}{PGA^2}\frac{PGA}{PGV} = \frac{I_E}{PGA \times PGV} \tag{3.2.5}$$

where PGA and PGV are the peak ground acceleration and peak ground velocity respectively, and I_E

$$I_E = \int_0^{t_E} \ddot{u}_g(t)^2 dt \tag{3.2.6}$$

where $\ddot{u}_g$ is the ground acceleration and t_E is the earthquake duration. I_E is proportional to the Arias Intensity.

The statistical analysis numerically defines n and x as follows:

$$n = 1 + 1.05\delta^{-1/3}\tau^{-2/3}(R-1)^{4/5} I_D^{4/5} \tag{3.2.7}$$

$$x = 0.17\delta^{1/6}\tau^{1/6}(R-1)^{-1/5} I_D^{1/5} \tag{3.2.8}$$

where

$$\tau = T/T_1 \qquad T \le T_1, \qquad \tau = 1 \qquad T > T_1$$

$$\delta = \xi/\xi_0 \qquad \xi \ge \xi_0, \qquad \delta = 1 \qquad \xi < \xi_0$$

Substituting the expressions of n and x in Eq. 3.2.4, n_{eq} can be expressed as

$$n_{eq} = 1 + 0.18(R-1)^{3/5} I_D \delta^{-1/6}\tau^{-1/2} \tag{3.2.9}$$

In the case of damping equal to 5 per cent and in the medium and long periods ranges Eq. 3.2.9 becomes

$$n_{eq} = 1 + 0.18(R-1)^{3/5} I_D \tag{3.2.10}$$

It can be noticed that Eq. 3.2.9 and Eq. 3.2.10 are linearly dependent on earthquake characteristics via the seismic index I_D. Consequently, I_D can be regarded as an indicator of the cyclic demand of the earthquake. Low values of I_D are obtained from impulsive earthquakes whereas high values of it are obtained from the earthquakes with long duration.

3.2.3 The Assessment of the Hysteretic Energy

An expression of the dissipated energy is obtained from the definition of the number of equivalent cycles n_{eq} and the reduction factor R as below:

$$\frac{E_h}{m} = (\mu_c - 1) n_{eq} \left(\frac{S_a(T)}{\omega} \right)^2 \left(\frac{1}{R} \right)^2 \tag{3.2.11}$$

where μ_c is the cyclic ductility, $\mu_c = 1 + \Delta u_{\max} / u_y$, and ω is the angular frequency of the system.

In an approximate way, Eq. 3.2.11 enables us to construct the hysteretic energy spectra by using the elastic spectrum S_a and defining proper expression of the reduction factor R.

As a result of extensive studies related to R, following expression is available for the case of rock and low-depth grounds:

$$R = 1 + 1.5(\mu - 1)^{4/5} \tau^{-3/4} \tag{3.2.12}$$

In evaluating the peak demand of hysteretic energy, another important parameter, because the period of peak demand generally takes place in the field of the medium periods, it is coincident with the peak value of pseudo-velocity S_a / ω. Combining Eq. 3.2.9, Eq. 3.2.11 and Eq. 3.2.12, the amount of the maximum hysteretic energy for a proportional damping ξ equal to 0.05 is defined by

$$\left(\frac{E_h}{m} \right)_{\max} = \frac{(\mu_c - 1)}{[1 + 1.5(\mu_c - 1)^{4/5}]^2} (1 + 0.23 I_D \sqrt{\mu_c - 1}) \left(\frac{S_a(T)}{\omega} \right)^2_{\max} \tag{3.2.13}$$

A simplified formulation of Eq. 3.2.13 can be obtained as

$$\left(\frac{E_h}{m} \right)_{\max} = 0.32 \left(\frac{\sqrt{\mu_c - 1}}{\mu_c} + 0.23 I_D \frac{\mu_c - 1}{\mu_c} \right) \left(\frac{S_a(T)}{\omega} \right)^2_{\max} \tag{3.2.14}$$

3.2.4 The Evaluation of Input Energy

The input energy imparted to a structure during an earthquake is mainly defined by the elastic period of the structure and the seismic characteristics of the ground motion, whereas it is hardly sensitive to the viscous damping and the previously mentioned characteristics of the inelastic response like the hysteresis and the ductility. However, the hysteretic energy forms the starting point for the estimation of the input energy.

Based on the seismic response of the SDF systems, it is observed that the relation between the hysteretic energy E_h and the input energy E_i is only sensitive to the demanded ductility and it is not significantly dependent on the seismic characteristics of the ground motion. The statistical analysis conducted in this issue provides us the following expression of this ratio for $\xi = 0.05$:

$$\frac{E_h}{E_i} = 0.72\frac{\mu_c - 1}{\mu_c} \tag{3.2.15a}$$

$$\frac{E_i}{m} = 1.4\frac{\mu_c}{\mu_c - 1}\frac{E_h}{m} \tag{3.2.15b}$$

A formulation of the input energy as a function of the cyclic ductility μ_c can be obtained from E_h / E_i ratio and Eq. 3.2.13 i.e.

$$\frac{E_i}{m} = 1.4\mu_c n_{eq}\left(\frac{S_a(T)}{\omega}\right)^2\left(\frac{1}{R}\right)^2 \tag{3.2.16}$$

This expression implies that the input energy spectra can be obtained from the pseudo-velocity spectrum by an approximate approach.

Furthermore, the maximum value of the input energy can be expressed, similarly with the expression of the dissipated energy, for $\xi = 0.05$ as

$$\left(\frac{E_i}{m}\right)_{\max} = 1.4\frac{\mu_c}{[1+1.5(\mu_c - 1)^{4/5}]^2}(1 + 0.23 I_D\sqrt{\mu_c - 1})\left(\frac{S_a(T)}{\omega}\right)^2_{\max} \tag{3.2.17}$$

Finally, the following simplified expression is obtained by using the approximate formulation of E_h:

$$\left(\frac{E_i}{m}\right)_{\max} = 0.45\left(\frac{1}{\sqrt{\mu_c - 1}} + 0.23 I_D\right)\left(\frac{S_a(T)}{\omega}\right)^2_{\max} \tag{3.2.18}$$

It is worth noting that the input energy E_i in this formulation is lesser sensitive to the possible ductility. Consequently, neglecting the influence of the ductility on E_i, assuming a ductility $\mu_c = 2$ which is the minimum value accepted in the statistical analysis, more simplified expression can be obtained from Eq. 3.2.18 as

$$\left(\frac{E_i}{m}\right)_{\max} = 0.45\left(1 + 0.23 I_D\right)\left(\frac{S_a(T)}{\omega}\right)^2_{\max} \tag{3.2.19}$$

3.2.5 A Comparison of Different Expressions for the Input Energy Demand

The expression of the peak input energy Eq. 3.2.19 can be written in the form

$$\left(\frac{E_i}{m}\right)_{\max} = 0.45\left(\frac{S_a(T)}{\omega}\right)^2_{\max} + 0.10 I_D\left(\frac{S_a(T)}{\omega}\right)^2_{\max} \tag{3.2.20}$$

The first term of Eq. 3.2.20 represents the amount of energy corresponding to the maximum impulse of the ground motion and is similar to Housner's assumption which is valid for the undamped system:

$$\left(\frac{E_i}{m}\right)_{\max} = \frac{1}{2}\left(\frac{S_a(T)}{\omega}\right)^2_{\max}. \tag{3.2.21}$$

The second term of it dependent on the seismic index I_D represents the influence of the earthquake duration.

Based on the other researches, another comparison is possible for the range of medium periods as

$$\left(\frac{S_a(T)}{\omega}\right)_{\max} = AV \cdot PGV \approx 2.5 PGV \tag{3.2.22}$$

where AV is the amplification spectral factor. Eq. 3.2.20 then takes the form

$$\left(\frac{E_i}{m}\right)_{\max} = 2.81PGV^2 + 0.63I_D PGV^2. \tag{3.2.23}$$

Substituting the expression of I_D in Eq. 3.2.23,

$$\left(\frac{E_i}{m}\right)_{\max} = 2.81PGV^2 + 0.63I_E \frac{PGV}{PGA} \tag{3.2.24}$$

The second term of Eq. 3.2.24 is similar to the formulation proposed by Kuwamura and Galambos, which is

$$\left(\frac{E_i}{m}\right)_{\max} = \frac{1}{8}T_g I_E \cong 0.54\frac{PGV}{PGA}I_E$$

where the predominant period of earthquake T_g, assumed to be equal to T_1, the limit period between the short and the medium period range, is offered the value $4.3(PGV/PGA)$.

For a medium cyclic demand, if the earthquake is characterized by I_D with the typical value 15, Eq. 3.2.24 takes the form

$$\left(\frac{E_i}{m}\right)_{\max} = 0.19I_D PGV^2 + 0.63I_D PGV^2 = 0.82I_E \frac{PGV}{PGA} \tag{3.2.25}$$

It is possible to express the seismic index I_D in a different form using the definition of effective duration by Trifunac and Brady and the dimensionless time variable t/t_d.

$$I_D = \frac{PGA}{PGV}\frac{1}{0.9}\frac{\int_{t_d}\ddot{u}_g^2(t)dt}{PGA^2} \approx 1.1t_d\frac{PGA}{PGV}\frac{\int_0^1\ddot{u}_g^2(t)d(t/t_d)}{PGA^2} \tag{3.2.26}$$

Substituting Eq. 3.2.26 into Eq. 3.2.20, the input energy demand can be expressed as

$$\left(\frac{E_i}{m}\right)_{\max} = 0.45\left(\frac{S_a}{\omega}\right)_{\max}^2 + 1.1t_d\frac{PGA}{PGV}\frac{\int_0^1\ddot{u}_g^2(t)d(t/t_d)}{PGA^2}\left(\frac{S_a}{\omega}\right)_{\max}^2 \tag{3.2.27}$$

Consequently, it can be noticed that the input energy demand is really dependent on the effective duration, and functionally dependent on the product of the dimensionless Arias intensity and the ratio PGA/PGV .

3.3 Other Energy-Related Empirical Formulations

3.3.1 The Relation between Amplification Factor of Equivalent Velocity of Input Energy and the Strong Motion Duration

Recalling Eq. 3.1.9, the amplification factor Ω_v of an input energy equivalent velocity spectrum for a given ductility ratio μ and a viscous damping ratio ξ can be rewritten as

$$\Omega_v(\mu,\xi) = \frac{v_{e(\max)}(\mu,\xi)}{\dot{u}_{g(\max)}} \tag{3.3.1}$$

Numerous statistical study shows that Ω_v and t_d are linearly dependent and the following equation is obtained by the least-squares method:

$$\Omega_v(\mu=5,\xi=0.05) = 1.0 + 0.12t_d \tag{3.3.2}$$

where the strong ground motion duration t_d is defined by Eq. 3.1.12.

Therefore, it is possible to assume the maximum energy input to a structure with a specified ratio if the strong motion duration for a given earthquake is known. Generally, the maximum input energy occurs in the immediate vicinity of the predominant period of the earthquake ground motion [6].

3.3.2 Formulations of Input Energy Proposed by Kuwamura and Galambos

Predominant period of the ground motions is given by

$$T_1 = 4.3\frac{\dot{u}_g}{\ddot{u}_g} \tag{3.3.3}$$

where $\dot{u}_g$ and $\ddot{u}_g$ are the peak ground velocity and acceleration [11].

a) The input energy at the end of the ground motion per unit mass is estimated by

$$\frac{E_i}{m} = \frac{1}{8} T_1 \int_0^{t_0} \ddot{u}_g(t)^2 dt \tag{3.3.4}$$

where t_0 is the complete ground motion.

b) A modified formula for input energy per unit mass is proposed as

$$\frac{E_i}{m} = 0.85 \frac{\dot{u}_g}{\ddot{u}_g} \int_0^{t_0} \ddot{u}_g(t)^2 dt \tag{3.3.5}$$

c) The maximum input energy per unit mass is estimated by the formula

$$\frac{E_i}{m} = 2.2 t_d^{0.5} \dot{u}_g^2 \tag{3.3.6}$$

where t_d is the duration of strong ground motion in seconds defined by Eq. 3.1.12.

d) Based on observations obtained in the parametric study, the following values are proposed as an upper bound for the hysteretic to input energy ratio:

$\frac{E_h}{E_i} = 0.8$ for 5 percent damping

$\frac{E_h}{E_i} = 0.9$ for 2 percent damping

PART 4 ENERGY-BASED SEISMIC DESIGN OF STRUCTURES

As mentioned in the previous parts, utilizing the energy concept in structural analysis has crucial meaning for the convenience in the seismic designing new structures, retrofitting existing structural facilities and the reliable damage assessment. This part is devoted to the preliminary presentation on energy-based seismic design of structures. As can be estimated, a comprehensive coverage of the topic is beyond the scope of this study.

4.1 Introduction

Two essential factors, demand and supply, forming the basic design equation are needed to be defined in seismic analysis of structures. The basic design equation can be interpreted as

demand	≤	supply
on		of
stiffness,		stiffness,
strength,		strength,
stability,		stability,
energy absorption and energy		energy absorption and energy
dissipation capacities		dissipation capacities [14].

Evaluation of the demand is related to the loading effect on structures while the estimation of the supply is related to the characteristics of the structure. Therefore, proper determination of loading effect is a fundamental step in seismic analysis. In the seismic resistant design, earthquake excitation is accepted as the loading effect. Reliable establishment of the design earthquakes comes next. It is necessary to reliably assess the damage potential of all the possible earthquake ground motions that can occur at the site

of the structure. Currently, the Safety or Survival-Level Design Earthquake is defined through Smoothed Inelastic Design Response Spectra (SIDRS). Most of the SIDRS used in seismic codes have been obtained directly from Smoothed Elastic Design Response Spectra (SEDRS) by using the displacement ductility ratio μ or the reduction factor R. SIDRS can be obtained directly as the mean or the mean plus one standard deviation of the Inelastic Response Spectra (IRS), corresponding to all the different time histories of the severe ground motions induced at the given site from possible earthquakes.

This approach is necessary for successful design for safety. However, it is not sufficient to avoid collapse and/or serious damage that can endanger human life. Although the IRS includes the effects of duration of strong motion at certain level, these spectra do not provide us the reliable information of the amount of energy due to be dissipated by whole structural system by means of hysteretic behavior during the critical ground motion. Only the value of maximum global ductility demand is expected from them. In other words, the maximum global ductility demand by itself does not give an appropriate definition of the damage potential of ground motions. As demonstrated in the previous parts, a more reliable and stable parameter than those currently used in assessing damage potential is the input energy E_i. For the rational earthquake-resistant design procedures, however, it is necessary to build the damage criteria on the simultaneous consideration of E_i, μ and the E_h [14].

4.2 Advantages of Using Energy Concept in Seismic Design of Structures

In addition to the conveniences of using energy concept in seismic analysis of structures explained in the previous parts, it has the following fundamental advantages. Absolute energy equation is written as

$$E_i = E_e + E_D \tag{4.2.1}$$

$$E_i = E_k + E_s + E_d + E_h \tag{4.2.2}$$

where E_e and E_D can be considered as the stored elastic energy and the dissipated energy respectively. If the design equation is recalled, this equation clearly explains that E_i represents the demands, and the summation $E_e + E_D$ represents the supplies. Eq. 4.2.1 apparently postulates that the first step for conducting an efficient seismic design is to estimate the E_i for the critical ground motion correctly; the second step is to analyze if it is possible to balance this demand with just the elastic response of the structure to be designed or it is proper to attempt to dissipate as much as possible amount of the E_i by means of E_D. As shown by Eq. 4.2.2, there are three ways of increasing E_D: The first is to increase linear viscous damping energy E_d; the second is to increase the hysteretic energy E_h; and the third is a combination of increasing E_d and E_h. For the time being, it is usual application to just attempt to increase E_h as much as possible through inelastic (plastic) behavior of the structure which means damage of the structural members. Recently it has been recognized that it is possible to efficiently increase the E_d and the control damage using Energy Dissipation Devices.

If it is hard to technically and/or economically balance the required input energy E_i through either E_e alone or $E_e + E_D$, it is possible to attempt to control (decrease) the E_i to the structure by applying Base Isolation Techniques. A combination of controlling (decreasing) the E_i by base isolation techniques and increasing the E_D by using energy dissipation devices is very optimal strategy not only for achieving efficient seismic-resistant design and construction, but also for the retrofitting of existing hazardous structures. To reliably use this energy approach, it is crucial to select the critical ground motion (design earthquake) which controls the design, in other words, the ground motion that has the largest damage potential for the structure to be designed. However, many parameters have been and are being used to decide design earthquakes, most of which are not reliable for assessing the damage potential of ground motions. As mentioned in the introduction, a suitable parameter for assessing damage potential of these motions is the E_i [14].

4.3 Design Principles

It is possible to define each earthquake-resistant design limit using energy balance concept. Based on the energy equation, the condition under which a structure can remain almost elastic is

$$E_{es} \geq E_{ed} = E_i - E_d - E_h \tag{4.3.1}$$

where E_{es} is the elastic energy supply and E_{ed} is the elastic energy demand.

The collapse limit of the structure is defined as

$$E_{hs} \leq E_{hd} = E_i - E_d - E_e \tag{4.3.2}$$

where E_{hs} is the hysteretic energy supply and E_{hd} is the hysteretic energy demand.

The condition under which the structure can survive without collapse is

$$E_{hs} \geq E_{hd} \tag{4.3.3}$$

A required performance level of the structures can be defined based on the comparison of corresponding quantity of energy supply and demand [1].

4.4 A Procedure for Energy-Based Seismic Design of Structures Using Yield Mechanism and Target Drift

In this section, a procedure for seismic design forces for multistory moment frame structures is presented using the energy balance concept. The energy balance concept which is used for constructing inelastic design response spectra for single-degree-of-freedom systems is modified and extended to cover the effects of plastic yield mechanism and the distribution of seismic forces along the height of the structure [12].

4.4.1 Review of Energy Balance Concept

The energy balance concept used in this study is based on the assumption that the energy needed to push a structure monotonically up to the maximum target deformation is equal

to the maximum earthquake input energy of an equivalent elastic system E_i which can be estimated by $\frac{1}{2}mS_v^2$ where S_v is the pseudovelocity. This concept is illustrated in Fig. 4.1. Generally, using the energy balance concept in deriving inelastic response spectra for elastoplastic systems from the elastic response spectra for the given values of displacement ductility factor keeps the results on the conservative side except that the structure has a very short period.

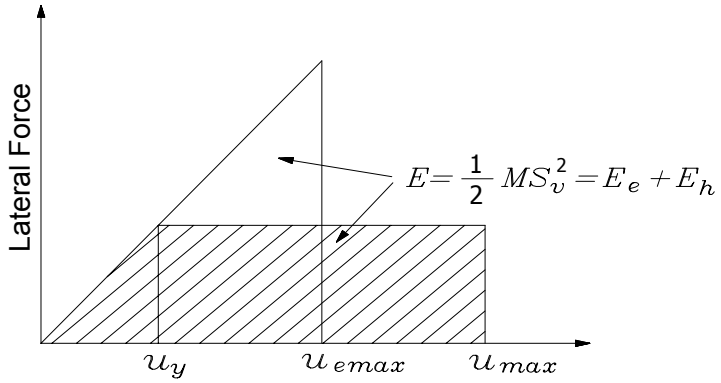

Figure 4.1 Energy balance concept

4.4.2 Energy Balance Concept in Multistory Frames

On a multistory structure with one-bay moment frame and a defined global mechanism shown in Fig. 4.2, the plastic deformation of the frame occurs after the structure reaches its yield point. In the plastic deformation range, it is assumed that the drift of the frame is uniform over the height of the structure and all of the energy is dissipated only in the plastic hinges. The inelastic story drift can be approximated by the plastic rotation of the frame θ_p. It is assumed that the energy balance concept is valid for such structures after the energy components are estimated properly.

Housner showed that the pseudovelocity spectra of typical earthquakes tend to remain practically constant over a wide range of periods. This is particularly valid for a spectrum obtained by averaging several response spectra of earthquakes with similar intensities. Based on this assumption, Housner showed that the maximum earthquake input energy for a MDF system, on the average, can be approximated by

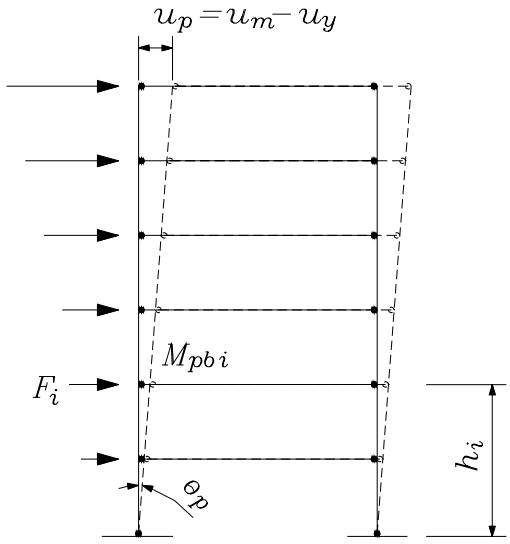

Figure 4.2 One-bay frame with global mechanism

$$E_i = \frac{1}{2} M S_v^2 = \frac{W g a^2 T^2}{8\pi^2} \tag{4.4.1}$$

where M is the total system mass, S_v is the pseudovelocity from the elastic response spectrum, a is the normalized pseudoacceleration with respect to the acceleration due to gravity g, W is the weight and T is the fundamental period.

Although Eq. 4.4.1 presents an approximate approach for the estimation of input energy, its accuracy is at acceptable level for the seismic design purposes. As known, the determination of precise energy demand requires an impractical calculation procedure based on the exact characteristics of the structure as well as the exact ground motion to be considered in the analysis. Nonetheless, a more comprehensive analysis may be needed in the case the structure is subjected to ground motions with much more different properties than that of earthquakes such as El Centro which was used in the derivation of the above equation.

Another important component of the energy balance equation is the elastic energy E_e. In the approximation of E_e, for an equivalent single-degree-of-freedom system, an empirical formulation has been proposed by Akiyama and Kato as

$$E_e = \frac{1}{2} M \left(\frac{T}{2\pi} \frac{V_y}{W} g \right)^2 \tag{4.4.2}$$

where V_y is the yield base shear.

Based on Eq. 4.4.1 and Eq. 4.4.2, total plastic or hysteretic energy E_h needs to be dissipated during the entire ground motion can be obtained from subtracting Eq. 4.4.2 from Eq. 4.4.1, that is

$$E_h = \frac{WT^2 g}{8\pi^2} \left[a^2 - \left(\frac{V_y}{W} \right)^2 \right] \tag{4.4.3}$$

The plastic energy formulated by Eq. 4.4.3 is equal to the energy dissipated through plastic hinges in the structure shown in Fig. 4.3. The proposed yield mechanism of the structure in Fig. 4.3 is expressed as

$$E_h = \left(\sum_{i=1}^{n} 2M_{pbi} + 2M_{pc} \right) \theta_p \tag{4.4.4}$$

where M_{pbi} is the plastic moment of the beam at level i and M_{pc} is the plastic moment of the columns at the base of the structure. Furthermore, the equivalent inertia forces must be in equilibrium with the internal forces after yielding. The internal work done in plastic hinges is equal to the external work done by the equivalent inertia forces, that is

$$\sum_{i=1}^{n} 2M_{pbi} + 2M_{pc} = \sum_{i=1}^{n} F_i h_i \tag{4.4.5}$$

where F_i is equivalent inertia force at level i and h_i is the height of beam level i from the ground. Assuming an inverted triangular force distribution, the inertia force at level i can be related the base shear by

$$F_i = \frac{w_i h_i}{\sum_{j=1}^{n} w_j h_j} V_j \tag{4.4.6}$$

where w_i (or w_j) is the weight of the structure ate level i (or j). Above assumed distribution shape of the force corresponds to the assumed linear shape of the first mode of vibration for a structure with global (strong column) yield mechanism.

Using Eq. 4.4.4, Eq. 4.4.5 and Eq. 4.4.6, Eq. 4.4.3 can be written as

$$\frac{V_y}{W}\left(\frac{\sum_{i=1}^{n} w_i h_i^2}{\sum_{i=1}^{n} w_i h_i}\right)\frac{\theta_p 8\pi^2}{T^2 g} = \left[a^2 - \left(\frac{V_y}{W}\right)^2\right] \tag{4.4.7}$$

Solving Eq. 4.4.7 for $\frac{V_y}{W}$, the solution of the above equation gives

$$\frac{V_y}{W} = \frac{-\alpha + \sqrt{\alpha^2 + 4a^2}}{2} \tag{4.4.8}$$

where α is a dimensionless parameter which depends on the stiffness of the structure, its modal properties and the intended plastic drift, and is given by

$$\alpha = \left(\frac{\sum_{i=1}^{n} w_i h_i^2}{\sum_{i=1}^{n} w_i h_i}\right)\frac{\theta_p 8\pi^2}{T^2 g} \tag{4.4.9}$$

Now it is possible to define the design base shear by Eq. 4.4.8 demanded by a design plastic drift level of the frame θ_p. After the base shear has been obtained, the design force corresponding to each level can be defined by Eq. 4.4.6.

Practically, the total target story drift of the structure, the combination of the elastic and plastic story drifts, is accepted as the base for an optimal design. Therefore, firstly, it is necessary to define the elastic drift of the structure at yield. For example, for a structure to be designed, if the estimated yield drift is 1%, and the maximum total drift is 3%, the plastic drift then can be defined as 2% (0.02).

It should be noted that the above procedure is based on the assumption that the plastic deformation of the frame is unidirectional and it only takes place during the peak deformation. Although it is unlikely the practical case, two research results below support the assumption.

Firstly, it has been proved that the interstory drift, which is a suitable damage index for frame structures, is generally larger than the global (roof) drift assumed in the design process. A study conducted by researchers shows that the interstory drift can be as larger as 30% than the global drift in reinforced concrete structures. The ratio between interstory drift and the global drift can increase up to 1.4 usually and, for some cases, even 2.0 for steel structures.

Secondly, it has been shown that the response of a single-degree-of-freedom system induced by the largest earthquake acceleration impulse properly represents the inelastic seismic response in a certain period range. The equivalent impulsive loading produces mainly unidirectional plastic deformation. Therefore, the unidirectional plastic drift representation could give reasonable results in the design procedure. This case is especially valid for near field earthquakes.

4.4.3 Design Provisions

4.4.3.1 Seismic Design Forces Based on the Spectral Acceleration in Turkish Code-1997

Based on the elastic design pseudoacceleration spectra proposed by many building codes, the design input energy level can be estimated by Eq. 4.4.1 in design procedures. Consequently, the spectral acceleration coefficient in Turkish Code-1997 which corresponds to the normalized pseudoacceleration in Eq. 4.4.1 can be used to evaluate the design input energy level. The spectral acceleration coefficient is given by

$$A(T) = A_0 IS(T) \tag{4.4.10}$$

where A_0 is the effective ground acceleration coefficient defined depending on the seismic zone, I is the building importance factor and $S(T)$ is the spectrum coefficient.

4.4.3.2 Plastic Design of Multistory Frames Based on Proposed Energy Concept

In the conventional design procedure, in which the distribution of internal forces is defined by the elastic analysis, the formation of undesirable mechanism may occur. Consequently, that case can result in unexpected failure mechanism after the formation

of beam hinges which is much different from that predicted. Therefore, in energy-based design of structures, the plastic design is more suitable as the primary design methodology. In this section, a simple procedure for the derivation of the design forces based on the assumption that the selected yield mechanism is maintained during the entire excitation as shown in Fig. 4.2.

Considering the n-story frame in its mechanism state shown in Fig. 4.2, the moment equilibrium equation of the frame can be rewritten as

$$\sum_{i=1}^{n} F_i h_i = \sum_{i=1}^{n} 2\beta_i M_{pbr} + 2M_{pc} \tag{4.4.11}$$

where F_i is the known design force at level i obtained as explained earlier, h_i is the height of the beam level i from the ground, β_i is the proportioning factor for the beam strength at level i, M_{pbr} is the common reference plastic moment for beams and M_{pc} is the required plastic moment of columns of in the first story. The beam proportioning factor β_i represents the relative beam strength at level i with respect to a reference plastic moment M_{pbr}. The product $\beta_i M_{pbr}$ is the plastic moment capacity of the beam at level i.

Properly estimating the values of β_i and M_{pc}, the design can be performed by obtaining the only unknown variable M_{pbr}. The determination of the beam proportioning factor β_i will be discussed later. The value of M_{pc} should be defined so as to eliminate a soft story mechanism in the first story. As an approach, assuming plastic hinges at the base and the top of the first story column, the required plastic moment capacity of the first story columns in one-bay frame should be

$$M_{pc} = \frac{1.1 V_y h_1}{4} \tag{4.4.12}$$

where V_y is the total base shear, h_1 is the height of the first story and the factor 1.1 is the overstrength factor to account for possible overstrength due to strain hardening.

After obtaining M_{pbr}, the required nominal beam strength at each level can then be determined as

$$\phi M_{pbi} \geq \beta_i M_{pbr} \tag{4.4.13}$$

where ϕ is the resistance factor and M_{pbi} is the nominal plastic moment capacity of the beam at level i.

Now it is possible to design the columns as a cantilever subjected to lateral forces and moments provided that the dimensions of the beams are defined. In order to realize a strong-column-weak-beam yield mechanism, the columns are needed to be designed on the assumption that the beams are fully strain hardened when the complete mechanism occurs. The overstrength factor ξ is introduced to increase the moment of a fully strain hardened beam so as to reach the goal of the strong-column-weak-beam yield mechanism.

The design moment of the columns at ultimate state can be estimated provided that the overstrength factor ξ is assigned by a proper value. Considering the corresponding term of Turkish Code-1997, the overstrength factor ξ can be assigned by 1.20 [15]. However, for the beam at the roof level, ξ can be equal to 1 because the global behavior at mechanism state is not much influenced by the plastic hinges allowed at that level.

4.4.3.3 Distribution of Beam Strength

As mentioned previously, the relative strength at each level represents the variation of story strength and stiffness over the height of the structure. The proper choice of the beam proportioning factor ξ_i ensures that the uniform maximum story drift along the height is realized and the input energy is evenly dissipated throughout the structure preventing concentrations of damage in any particular part of the structure.

The criteria to be considered in defining the distribution of beam strengths should be the best representation of the story shears generated from a variety of earthquakes. This will ensure that the stories with relatively low-input story shears have relatively small

strength and stiffness; similarly, the stories with relatively high-input story shears have relatively large strength and stiffness.

As a first approach, the relative distribution of earthquake induced story shears can be represented by a function of the relative distribution of static story shears obtained from the assumed linear force distribution represented by Eq. 4.4.6. The actual ratio of the earthquake induced story shear at any level i to that at the top level n is assumed to be in the form

$$\beta_i = \left(\frac{V_i}{V_n} \right)^b \tag{4.4.14}$$

where V_i and V_n are the static story shears at level i and the top story obtained from linearly distributed design forces given by Eq. 4.4.6 respectively, b is a numerical factor to be determined. This factor can be best estimated by using the least-squares fit of the actual shear distributions under representative ground motions of a given site.

In order to determine the optimum variation of beam strengths along the height of the frames, a study has been conducted assigning 0.25, 0.50, 0.75 and 1.0 to b respectively for a six-story moment frames. It has been shown that the variation of beam strengths along the height influences the response of these frames significantly. After performing the necessary calculation and the least-square fitting procedure on the related data, the factor b has been obtained as 0.527. For practical purposes, the rounded value of 0.50 was selected. It should be noted that this value of b may not be applicable to all cases due to the uncertain nature of earthquakes. It is assumed in the research study [12] that the four earthquakes, El Centro 1940, Northridge 1994 (Sylmar Station), Northridge 1994 (Newhall Station) and a synthetic ground motion which were used in the study, are representative of the earthquakes at a given site.

4.4.3.4 Verification of the Proposed Energy Concept

A series of nonlinear analysis including both inelastic static and inelastic time history analysis were conducted by the author in order to verify the proposed procedure. The results show that the strong-column-weak-beam is maintained on all frames subjected to

the study and the yield drifts are in the predicted range. Generally, the results of the study show that the proposed energy balance concept is most effective when used with structures with moderate heights and target story drifts. For other structures, the results are on the conservative side with the exception of the two-story frames where the results were rather unconservative.

4.4.3.5 Comparison with Existing Design Methodology

At present, classical seismic design approaches are traditionally established on the equivalent static force concept. The equivalent static design forces are obtained from the expected maximum seismic forces due to elastic behavior through some modifications depending on the ductility of the system. The members of the structure are then designed to resist the forces. Usually elastic structural analysis including either strength design or working stress design forms the base of this procedure. In the strength designing, the first significant yield level is considered as the level of forces. However, because an explicit check at the ultimate level is not performed, the behavior of the structure at the ultimate state can be significantly different from that proposed depending on the reserve strength and the failure mechanism. Clearly, if the reserve strength is less then that implicitly proposed by the code or the structure performs an unexpected mechanism, the response of the structure is affected correspondingly.

Contrarily, consideration of the structure at the ultimate (maximum deformation) state is the matter of issue in the proposed design procedure. A selected yield mechanism at ultimate state determines the inelastic design base shear. In another words, the base shear is determined based on a target maximum deformation using the energy balance concept. Thereby, the expected yield mechanism is maintained with sufficient strength conforming to a given ductility.

The design method introduced here can be suitably used as a general preliminary design procedure. It is possible to shorten the design iteration process aiming the capture of expected performance level. It is especially useful to apply this procedure when the performance-based design framework is concerned in which the structures are designed for multiple levels of seismic hazard each with different deformation criteria.

Finally, as a general procedure, it could be necessary to conduct more rigorous analysis such as nonlinear time-history analysis which covers structural irregularity, specific site effects and accurate damage evaluation of critical members.

4.4.4 Example

4.4.4.1 Analysis by the Proposed Energy Method

A six-story reinforced concrete structure with one-bay moment frame having the characteristics shown in Fig. 4.3 is analyzed. As shown in Fig. 4.3, the story height is 4.0m and the bay width is 7.0m. The story weight is given as 400kN. The dimensions of columns and beams are $0.40 \times 0.6m$ and $0.35 \times 0.60m$ respectively. The modules of elasticity of concrete $E = 3 \times 10^7 kN/m^2$. The inelastic drift θ_p is selected as 0.020 corresponding approximately to total target drift 3% assuming the yield drift 1%. The values needed to evaluate the spectral acceleration coefficient given in Turkish Code-1997 are selected as $A_0 = 0.4$ (seismic zone 1), $I = 1.0$ and $T_A = 0.15s$, $T_B = 0.60s$ (soil type S3). The fundamental period, the period of the first mode is estimated as $T = 0.92\,\text{sec}$ using SAP2000.

$$\alpha = \left(\frac{\sum_{i=1}^{n} w_i h_i^2}{\sum_{i=1}^{n} w_i h_i} \right) \frac{\theta_p 8\pi^2}{T^2 g} = 3.293$$

$T_A = 0.15s$, $T_B = 0.60s$, $T_1 = 0.92s$, $T_1 > T_B$

$$S(T) = 2.5(T_B / T)^{0.8} = 1.77$$

$$a = A(T) = A_0 I S(T) = 0.708$$

$$\frac{V_y}{W} = \frac{-\alpha + \sqrt{\alpha^2 + 4a^2}}{2} = 0.146$$

Distribution of the base shear and proportioning factor for beam strength are shown in Fig. 4.4.

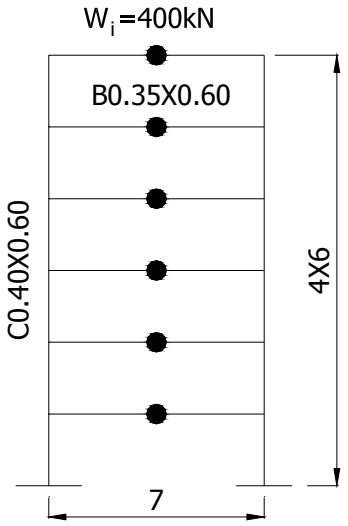

Figure 4.3 Six-story, one-bay reinforced concrete structure

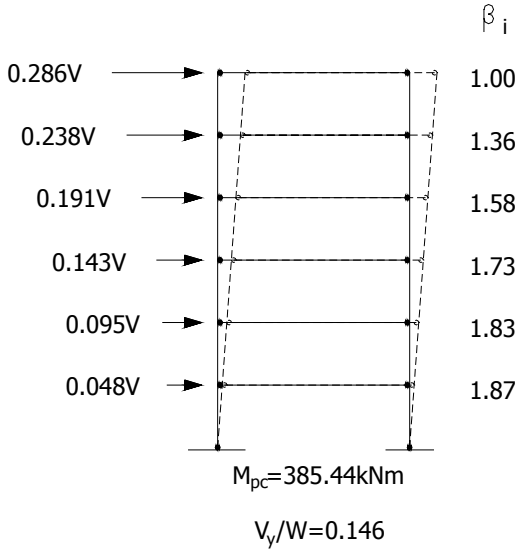

Figure 4.4 Distribution of the base shear and proportioning factor for beam strength

$$V_y = 0.146W = 350.4kN$$

$$M_{pc} = \frac{1.1V_y h_1}{4} = 385.44kNm$$

The shear force of a column is calculated as

$$F = \frac{V_y}{2} = 175.2kN$$

Solving Eq. 4.4.11 for the common reference plastic moment for beams M_{pbr} for a column is expressed as

$$M_{pbr} = \frac{\sum_{i=1}^{n} F_i h_i - M_{pc}}{\sum_{i=1}^{n} \beta_i} = 273.67kN$$

The values of plastic moment capacity of the beam at each level M_{pbi} are calculated using Eq. 4.4.13. Selecting the resistance factor $\phi = 1.15$ and the overstrength factor $\xi = 1.20$ except the roof level where 1 is selected, the values of the moment $\xi\phi M_{pbi}$ needed to determine the required plastic moment of columns are shown in Fig. 4.5. Plastic moment of columns can be computed using the moment equilibrium of hinges. In other words, the values of the moment $\xi\phi M_{pbi}$ are distributed on columns based on their rigidity.

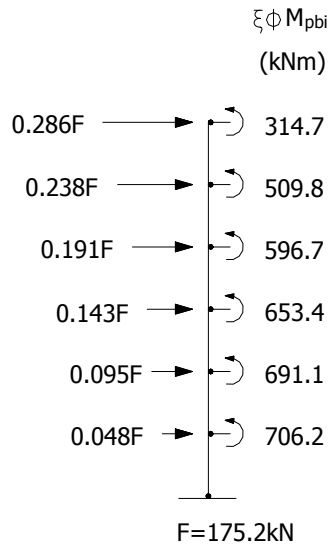

Figure 4.5 The plastic moment capacity of the beams

4.4.4.2 Analysis by the Equivalent Static Force Method of Turkish Code 1997

The spectral acceleration coefficient is given by

$$A(T) = A_0 IS(T) \tag{4.4.15}$$

where A_0 is the effective ground acceleration coefficient defined depending on the seismic zone, I is the building importance factor and $S(T)$ is the spectrum coefficient.

Total equivalent base shear is given by

$$V_t = WA(T_1)/R_a(T_1) \geq 0.10 A_0 IW \tag{4.4.16}$$

where W is the total building weight and R_a is the seismic load reduction factor. Total equivalent base shear is distributed along the elevation of the building based on the first mode shape as it is explained within the previously proposed energy-based seismic design method.

Seismic zone 1 $\rightarrow$ $A_0 = 0.4$, $I = 1$

Soil type 3 $\rightarrow$ $T_A = 0.15s$, $T_B = 0.60s$ $T_1 = 0.92s$, $T_1 > T_B$

$S(T) = 2.5(T_B/T)^{0.8} = 1.77$

$A(T) = A_0 IS(T) = 0.708$

$V_t = WA(T_1)/R_a(T_1) = 6 \times 400 \times 0.708/8 = 212.4kN$

where $R_a(T_1) = 8$ for the building with high ductility level.

Comparison of two methods:

Recalling the proposed energy-based seismic design method, total yield base shear is obtained as

$V_y = 0.146W = 350.4kN$.

In the equivalent static force method, total base shear is obtained as

$V_t = A(T_1)W/R_a = 212.4kN$ considering $R_a = 8$.

Based on the comparison of the two results, it can be observed that the value of the elastic force reduction factor R_a for the structure with high ductility level is slightly exaggerated. Using the result obtained from the example dedicated to the proposed energy method, a smaller value for R_a can be approximated as

$$R_a = A(T_1)W / V_y = 0.708 \times 2400 / 350.4 = 4.8 \approx 5$$

In the result, the elastic force reduction factor R_a can be more reasonably assigned by 5 or it might be necessary to conduct rigorous research on 8, the present value of R_a.

CONCLUSIONS

From this study dedicated to the energy concept and its effective usage in seismic analysis, it is possible to make following conclusive remarks.

1. In traditional seismic analysis of structures in which the loading effect of the earthquake is represented by static equivalent forces, the effect of duration-related cumulative damage is neglected. Moreover, the loading effect of the earthquake and the resistance of the structure are coupled.

2. Duration-related cumulative damage can be taken into account using a stable parameter input energy as the loading effect, by which, similarly, the characteristics of ground motions and those of the structure can be dealt with separately which means that coupling is eliminated.

3. For both SDF systems and MDF systems, two kinds of energy equation, absolute energy equation and relative energy equation, are available depending on which one of total displacement and relative displacement is used.

4. Input energy is evaluated as the sum of kinetic energy, damping energy, strain energy and hysteretic energy. The energy quantities except the kinetic energy are uniquely defined.

5. For SDF systems, the significant difference in magnitude of E_i and E_i' can be observed for the long period structure, i.e. when $T > 5\,\text{sec}$.

6. In the extreme cases, $E_i = 0$ and $E_i' = \dfrac{m(\dot{u}_g)^2}{2}$ when $T \to \infty$; $E_i = \dfrac{m(\dot{u}_g)^2}{2}$ and $E_i' = 0$ when $T \to 0$.

7. It is also possible to evaluate the energy quantities of MDF systems using equivalent SDF system.

8. Seismic input energy demand on the structure is assumed to be related to the total power of the acceleration of the ground motion.

9. In order to determine the peak amplification factor of the equivalent input energy velocity spectrum, a spectral shape is proposed for the input energy spectrum.

10. Through statistical study, the average peak factor representing the relation between the peak-ground-acceleration and the root-mean-square of the ground acceleration is obtained to be about 4 in order to estimate the peak amplification factor.

11. It is noted that the peak amplification factor for the input energy spectrum depends on the peak-ground-acceleration to peak-ground-velocity ratio and duration of the strong motion phase of the ground motion.

12. By the proposed procedure, it is possible to estimate the hysteretic energy spectra and the input energy spectra using the knowledge of the pseudovelocity spectrum and the seismic index I_D characterizing the seismic input.

13. The proposed relations for E_h and E_i gives similar formulations proposed by other researchers.

14. The input energy E_i is a stable parameter to represent the loading effect. However, for the rational earthquake-resistant design procedures, it is necessary to build the damage criteria on the simultaneous consideration of E_i, μ and E_h.

15. Eq. 4.2.1 clearly explains that E_i represents the demands and the summation of $E_e + E_D$ i.e. the elastic energy plus the dissipated energy, represents the supplies. The basic design equation can be interpreted as the supply should be equal to or larger than the demand. An effective seismic design can be reached by increasing dissipated energy via energy dissipation devices or decreasing the input energy via base isolation techniques.

16. A required performance level of the structures can be defined based on the comparison of corresponding quantity of energy supply and demand

17. Type of yield mechanism is very important in defining the characteristics of multistory structures especially in the post yield range such as dominant mode shapes and ductility demand.

18. In the proposed seismic design procedure, the energy balance concept used in deriving inelastic design response spectra for SDF systems is modified and extended to include the plastic yield mechanism and the distribution of seismic forces along the height of the structure.

19. Design forces are obtained based on the selected target drift, a selected design pseudovelocity spectrum and a selected plastic yield mechanism.

20. Comparing the proposed energy-based seismic design method with the equivalent static force method of Turkish Code 1997 through a numerical example, it can be observed that the value 8 of the elastic force reduction factor R_a for the structure with high ductility level is slightly exaggerated. The elastic force reduction factor R_a can be more reasonably assigned by 5 or it might be necessary to conduct rigorous research on the present value of R_a.

REFERENCES

[1] Akiyama, H., Earthquake-Resistant Limit-State Design for Buildings, University of Tokyo Press, Tokyo, 1985.

[2] Benavent-Climent, A., Pujades, L. G. and Lopez-Almansa, F., Design Energy Input Spectra for Moderate-Seismicity Regions, Earthquake Engineering and Structural Dynamics, Vol. 31, pp. 1151-1172, 2002.

[3] Uang, C.-M. and Chou, C. C., Establishing Absorbed Energy Spectra-An Attenuation Approach, Earthquake Engineering and Structural Dynamics, Vol. 29, pp. 1441-1455, 2000.

[4] Manfredi, G., Evaluation of Seismic Energy Demand, Earthquake Engineering and Structural Dynamics, Vol. 30, pp. 485-499, 2001.

[5] Hori, N. and Inoue, N., Damaging Properties of Ground Motions and Prediction of Maximum Response of Structures Based on Momentary Energy Response, Earthquake Engineering and Structural Dynamics, Vol. 31, pp. 1657-1679, 2002.

[6] Uang, C.-M. and Bertero, V. V., Evaluation of Seismic Energy in Structures, Earthquake Engineering and Structural Dynamics, Vol. 19, pp. 77-90, 1990.

[7] Chopra, Anil K., Dynamics of Structures Theory and Applications to Earthquake Engineering, Prentice Hall International, Inc., New Jersey, 1995.

[8] Rodriguez, M., A Measure of the Capacity of Earthquake Ground Motions to Damage Structures, Earthquake Engineering and Structural Dynamics, Vol. 23, pp. 627-643, 1994.

[9] Chai Y. H., Fajfar P., A Procedure for Estimating Input Energy Spectra for Seismic Design, Journal of Earthquake Engineering, Vol. 4, pp. 539-561, 2000.

[10] Tso, W. K., Zhu, T. J. and Heidebrecht, A. C., Seismic Energy Demands on Reinforced Concrete Moment-Resisting Frames, Earthquake Engineering and Structural Dynamics, Vol. 22, pp. 533-545, 1993.

[11] Fajfar, P., Vidic, T. and Fischinger, M., On Energy Demand and Supply in SDOF Systems, Nonlinear Seismic Analysis and Design of Reinforced Concrete Buildings, Elsevier Applied Science, Amsterdam, pp 41-61, 1992.

[12] Leelataviwat, S., C. Goel, S. and Stojadinovic, B., Energy-Based Seismic Design of Structures Using Yield Mechanism and Target Drift, Journal of Structural Engineering, August, 2002.

[13] Chou, C. C., Uang, C. M., A Procedure for Evaluating Seismic Energy Demand of Framed Structures, Earthquake Engineering and Structural Dynamics, Vol. 32, pp. 229-244, 2003.

[14] Bertero, V. V. and Uang, C. M., Issues Future Directions in the Use of an Energy Approach for Seismic-Resistant Design of Structures, Nonlinear Seismic Analysis and Design of Reinforced Concrete Buildings, Elsevier Applied Science, Amsterdam, pp 3-21, 1992.

[15] Afet Bölgelerinde Yapılacak Yapılar Hakkında Yönetmelik, TMMOB İnşaat Mühendisleri Odası İstanbul Şubesi, İstanbul, 1997.

APPENDICES

Appendix A C Program for Elastic Response

```
/* Elastic Dynamic Response: Newmark's average acceleration method */
#include<stdio.h>
#include<math.h>
#include<conio.h>

void main(void)
{
 int i=0;
 int n=0;
 double t, deltap, deltap1, k1, deltau, u, udot, udoubledot;
 double deltaudot, deltaudoubledot, deltat;
 double p[6000];
 double m=10142.4, c=31847.136, k=10000000.0;
 double a, b;

FILE *fin, *fout;
if((fin=fopen("load.txt", "r"))==NULL)
 {
                printf("fin can not be opened.");
 }
 fout=fopen("result.txt", "w");

 while(!feof(fin))
            {
                        fscanf(fin,"%lf", p + n);
                        n++;
            }

      t=0.0, u=0.0, udot=0.0, deltat=0.005;
      a=(4/deltat)*m+2*c;
      b=2*m;
      udoubledot=(p[i]-c*udot-k*u)/m;
      deltap=p[i+1]-p[i];
      k1=k+(2/deltat)*c+(4/(deltat*deltat))*m;

      deltap1=deltap+a*udot+b*udoubledot;
      deltau=deltap1/k1;
      deltaudot=(2/deltat)*deltau-2*udot;
      deltaudoubledot=(4/(deltat*deltat))*(deltau-deltat*udot)-2*udoubledot;
```

```
fprintf(fout,"%15.6lf %15.6lf %15.6lf %15.6lf %15.6lf %15.6lf %15.6lf %15.6lf
%15.6lf %15.6lf\n", t, p[i], udoubledot, deltap, deltap1, deltau, deltaudot,
deltaudoubledot, udot, u);

      u=u+deltau;
      udot=udot+deltaudot;
      udoubledot=udoubledot+deltaudoubledot;

 for(i=1; i<5183; i=i+1)
          {
      t=t+0.005;
      deltap=p[i+1]-p[i];
      deltap1=deltap+a*udot+b*udoubledot;
      deltau=deltap1/k1;
      deltaudot=(2/deltat)*deltau-2*udot;
      deltaudoubledot=(4/(deltat*deltat))*(deltau-deltat*udot)-2*udoubledot;

fprintf(fout,"%15.6lf %15.6lf %15.6lf %15.6lf %15.6lf %15.6lf %15.6lf %15.6lf
%15.6lf %15.6lf\n", t, p[i], udoubledot, deltap, deltap1, deltau, deltaudot,
deltaudoubledot, udot, u);

      u=u+deltau;
      udot=udot+deltaudot;
      udoubledot=udoubledot+deltaudoubledot;
          }
 fcloseall();
}
```

Appendix B C Program for Inelastic Response

```
/* Inelastic Dynamic Response: Newmark's average acceleration method */
#include<stdio.h>
#include<math.h>
#include<conio.h>

void main(void)
{
 int i=0;
 int n=0;
 double t, fs, udoubledot, deltap, deltap1, k, k1, deltau, u, udot;
 double deltaudot;
 double p[6000];
 double m=10142.4, c=31847.136, deltat=0.005;
 double a, b;

FILE *fin, *fout;
if((fin=fopen("load.txt", "r"))==NULL)
```

```
 {
                printf("fin can not be opened.");
 }
 fout=fopen("result.txt", "w");

 while(!feof(fin))
          {
                    fscanf(fin,"%lf", p + n);
                    n++;
          }

     t=0.0, u=0.0, udot=0.0, udoubledot=0.0, k=10000000.0, fs=0.0;
     a=(4/deltat)*m+2*c;
     b=2*m;
     deltap=p[i+1]-p[i];
     deltap1=deltap+a*udot+b*udoubledot;
     k1=k+(2/deltat)*c+(4/(deltat*deltat))*m;
     deltau=deltap1/k1;

fprintf(fout,"%15.6lf %15.6lf %15.6lf %15.6lf %15.6lf %15.6lf %15.6lf %15.6lf
%15.6lf %15.6lf\n", t, p[i], fs, udoubledot, deltap1, k, k1, deltau, udot, u);

 for(i=1; i<5183; i=i+1)
        {
     t=t+0.005;
     fs=fs+k*deltau;
     u=u+deltau;
     deltaudot=(2/deltat)*deltau-2*udot;
     udot=udot+deltaudot;

  if (fs>=1636.0 && udot>=0.0 ||  fs<=-1636.0 && udot<=0.0)  k=0.0;
      else k=10000000.0;
  if (fs>1636.0) fs=1636.0;
  if (fs<-1636.0) fs=-1636.0;

     udoubledot=(p[i]-c*udot-fs)/m;
     deltap=p[i+1]-p[i];
     deltap1=deltap+a*udot+b*udoubledot;
     k1=k+(2/deltat)*c+(4/(deltat*deltat))*m;
     deltau=deltap1/k1;

fprintf(fout,"%15.6lf %15.6lf %15.6lf %15.6lf %15.6lf %15.6lf %15.6lf %15.6lf
%15.6lf %15.6lf\n", t, p[i], fs, udoubledot, deltap1, k, k1, deltau, udot, u);
        }
 fcloseall();
}
```

Appendix C Absolute E_d, E_h, E_s, E_k time history of the system with $T_n = 0.2s$

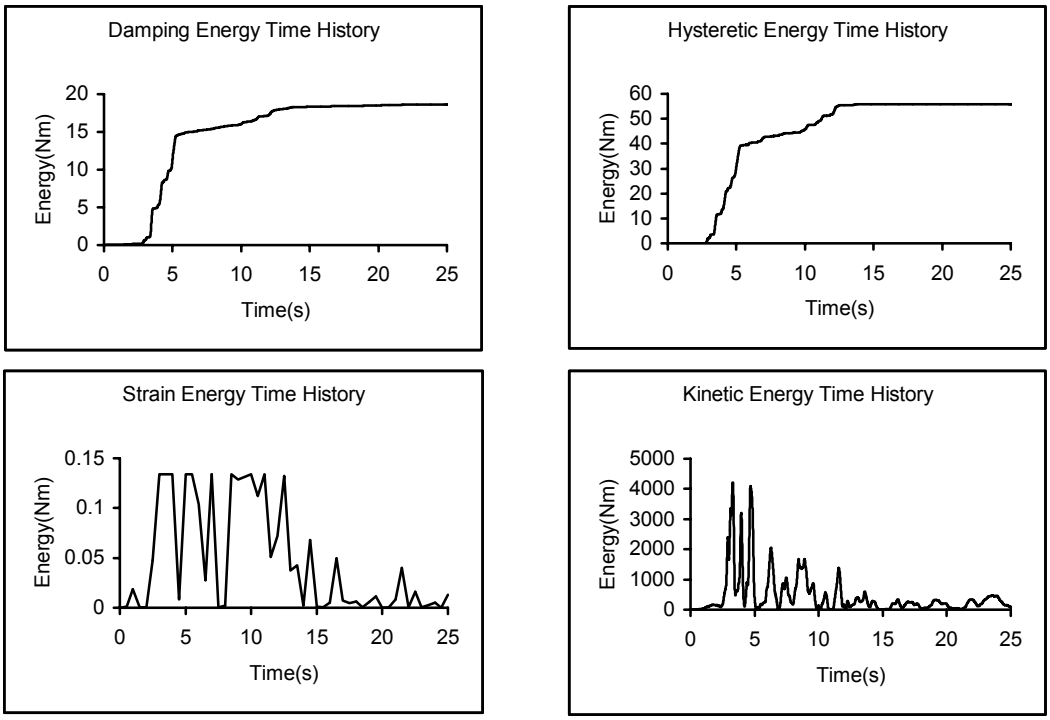

Appendix D Absolute E_d, E_h, E_s, E_k time history of system with $T_n = 5s$

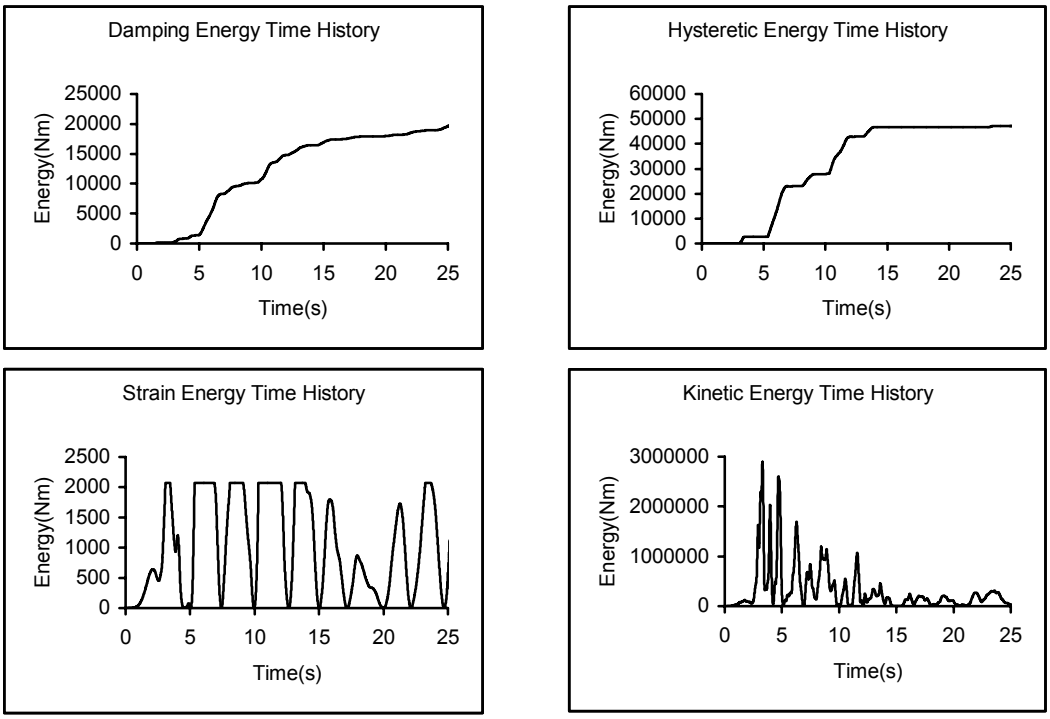

Appendix E Relative E_d, E_h, E_s, E_k' time history of the system with $T_n = 0.2s$

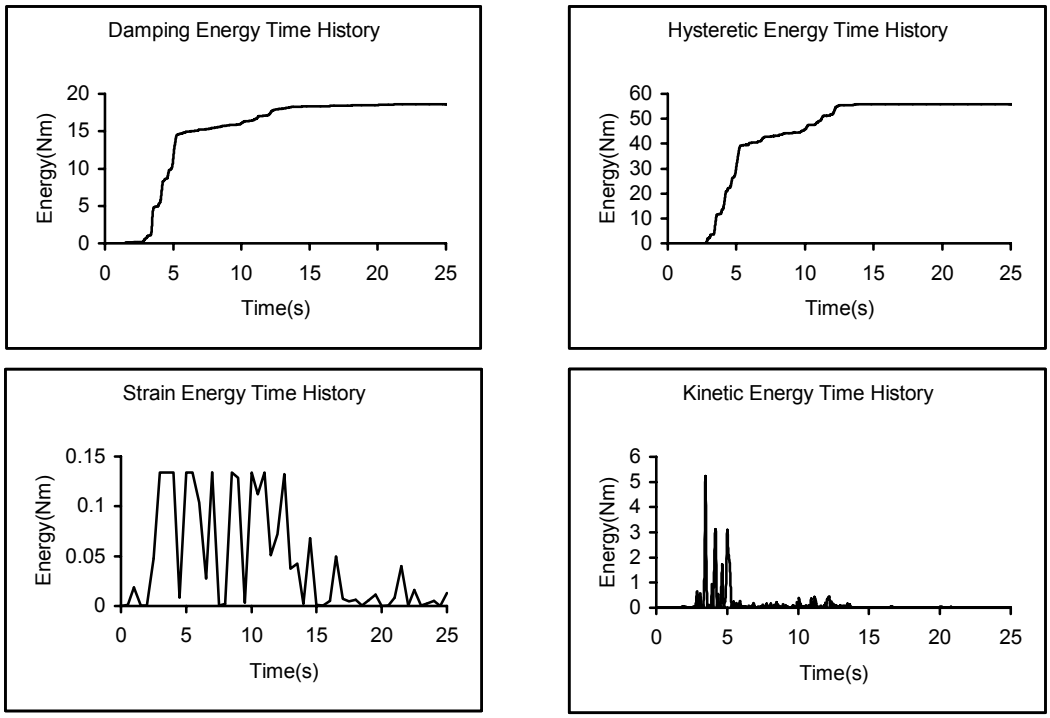

Appendix F Relative E_d, E_h, E_s, E_k' time history of the system with $T_n = 5s$

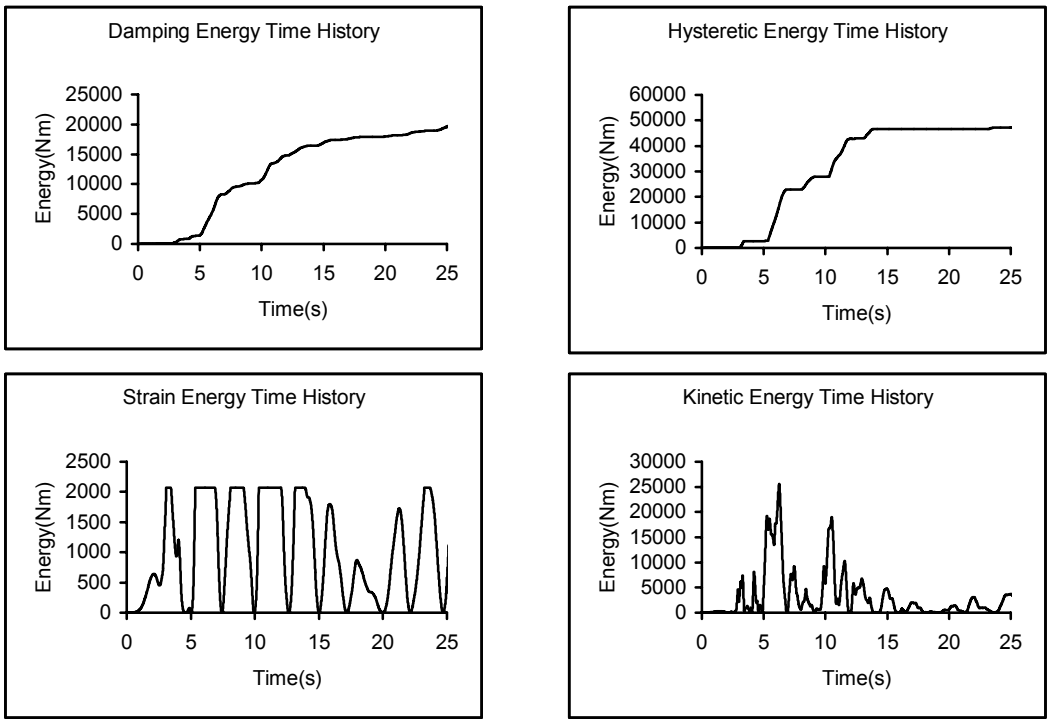

BIOGRAPHY

Ali Ruzi, an Uygur Turkish, was born in 1972 in Hoten, China. He graduated from the school of civil engineering, Urumçi Industrial Institute in 1992. He started master of structural engineering at İstanbul Technical University in February 2000.